1966

A study of the effect of magnetite additions to shell molds on the surface quality of low carbon steel castings

Robert C. Tooke

Department:

A STUDY OF THE EFFECT OF MAGNETITE ADDITIONS TO SHELL MOLDS ON THE SURFACE QUALITY OF LOW CARBON STEEL CASTINGS.

BY

ROBERT C. TOOKE - 1941

A

THESIS

submitted to the faculty of

THE UNIVERSITY OF MISSOURI AT ROLLA

in partial fulfillment of the requirements for the

Degree of

MASTER OF SCIENCE IN METALLURGICAL ENGINEERING

Rolla, Missouri

1966

Approved by

Lyle F. Ray (advisor) Fred Assbridge

R. F. Davidson A. H. Culp, Jr.

ABSTRACT

Shell molds containing additions of ten to fifty percent magnetite, Fe_3O_4, of various particle sizes were cured by induction heating. For comparison, regular shell molds were made using silica and zircon sand. Low carbon steel was cast into all of the molds.

Castings produced from the regular shell molds exhibited poor surfaces due to mold expansion. Magnetite additions eliminated the expansion defects from the casting surfaces.

Excellent surfaces were obtained on the low carbon steel castings with proper selection of the magnetite particle size and the percent of magnetite added. Improper combinations of size and amount of magnetite resulted in defects associated with the magnetite additions to the mold material.

ACKNOWLEDGEMENTS

The author wishes to express his sincere appreciation to Professor Robert V. Wolf of the Department of Metallurgical Engineering for his guidance, assistance, and encouragement during the course of this investigation. The author also takes this opportunity to thank Mr. Robert L. Wright, Instructor of Metallurgical Engineering for the many valuable contributions he made concerning this investigation.

The use of the facilities of the Oklahoma Steel Castings Company of Tulsa, Oklahoma, was extremely beneficial to this investigation. In particular, the author extends his gratitude to Messrs. Ed O'Brien, Carl Townsend, and Frank Skaggs of this Company for their cooperation.

TABLE OF CONTENTS

		Page
ABSTRACT		ii
ACKNOWLEDGEMENTS		iii
TABLE OF CONTENTS		iv
LIST OF ILLUSTRATIONS		vi
LIST OF TABLES		ix
I.	INTRODUCTION	1
II.	LITERATURE SURVEY	2
	A. Shell Molding	2
	B. Surface Defects	6
	C. Reactions between Iron Oxide and Silica	14
III.	EXPERIMENTAL PROCEDURE	21
	A. Preparation of Mold Materials	21
	B. Making of Molds	25
	C. Pouring and Analysis of Castings	33
IV.	RESULTS	40
	A. Introduction	40
	B. Expansion Defect	42
	C. Surface Beads	44
	D. Surface Blow	45
	E. Acceptable Surfaces	47
	F. Summary of Results	47
V.	DISCUSSION OF RESULTS	69
VI.	CONCLUSIONS	79
BIBLIOGRAPHY		81

Page

APPENDIX..... 85

I. Screen Analysis of Sands..... 86
II. Resin Content of Magnetite..... 90
III. Complete Description of Castings..... 93

VITA..... 96

LIST OF ILLUSTRATIONS

Figures — Page

1. Thermal expansion of silica..... 7
2. Stable phases of the system Fe-Si-O as a function of temperature and atmosphere..... 16
3. Equilibrium diagram of the system Fe-Fe_2O_3..... 18
4. Equilibrium diagram of the system FeO-SiO_2..... 19
5. Longitudinal section of mold (actual size)..... 26
6. Transverse sections of mold (actual size)..... 27
7. Photograph of three part pattern used to form mold cavity..... 29
8. Photographs of experimental apparatus..... 32
9. Representative photographs of finished molds..... 34
10. Effect of composition on appearance of finished molds..... 35
11. Preparation for and pouring of molds..... 37
12. Sample photographs of castings made for this investigation..... 39
13. Photographs of surfaces of castings poured in molds containing silica sand and +65 mesh magnetite..... 50
14. Photographs of surfaces of castings poured in molds containing silica sand and +100 mesh magnetite..... 51,52
15. Photographs of surfaces of castings poured in molds containing silica sand and +150 mesh magnetite..... 53

16. Photographs of surfaces of castings poured in molds containing silica sand and +200 mesh magnetite..... 54,55

17. Photographs of surfaces of castings poured in molds containing silica sand and +325 mesh magnetite..... 56

18. Photographs of surfaces of castings poured in molds containing silica sand and -325 mesh magnetite..... 57

19. Photographs of surfaces of castings poured in regular silica sand shell molds..... 58

20. Photographs of both surfaces of casting #41 made in composite mold..... 59

21. Photographs of surfaces of castings poured in molds containing zircon sand or zircon sand plus magnetite..... 60

22. Schematic representation of rough surface due to mold material expansion..... 61

23. Photomicrographs (100X) from casting #37 representative of the surface structure of castings exhibiting expansion defects.... 62

24. Photomicrographs (100X) of the surface on opposite sides of casting #41..... 63

25. Photomicrographs (100X) comparing surface structures in casting #6..... 64

26. Photomicrographs (100X) showing structure of surface beads..... 65

27. Photomicrographs (100X) of the surface structure of castings exhibiting the gas blow defect..... 66

28. Photomicrographs (100X) of the surface structure of castings exhibiting no surface defects..... 67

29. Rating of casting surfaces as a function of mold composition..... 68

30. Photographs of mold material (after casting) at metal interface..... 73

31. Equilibrium diagram of the system $FeO \cdot ZrO_2$..... 74

32. Model illustrating expansion in presence of liquid phase..... 76

33. Size distribution of sand grains..... 89

34. Variation of resin content with magnetite particle size..... 92

LIST OF TABLES

TABLE		PAGE
I.	Calculation of the AFS Grain Fineness Number of the Silica Sand.....	87
II.	Calculation of the AFS Grain Fineness Number of the Zircon Sand.....	88
III.	Results of the Determination of the Resin Content of Magnetite.....	91
IV.	Complete Description of Castings.....	93-96

I INTRODUCTION

A source of heat is required to cure the resin bond in shell molds. Conventional methods of curing shell molds involve contact of the mold material with a heated metal pattern. The results of recent research performed at the University of Missouri at Rolla indicate that shell molds can be cured by induction heating if powdered susceptors are present in the mold material. Additions of powdered magnetite to the mold material allow curing of the shell mold by induction heating.

Although the shell mold process offers many advantages in the production of castings, some difficulty has been experienced in obtaining the high quality surface expected on castings made in shell molds. Surface quality problems are most pronounced when low carbon steel is cast into shell molds; consequently, considerable research has been devoted to the prevention of surface defects on shell molded low carbon steel castings.

The purpose of this investigation was to evaluate the effect of powdered magnetite additions on the surface quality of low carbon steel castings which were produced from shell molds cured by induction heating.

II LITERATURE SURVEY

A. Shell Molding

"A metal casting is a shape obtained by pouring liquid metal into a mold or cavity and allowing it to freeze and thus to take the form of the mold."[1] Cores are inserted into the mold to form contours of casting which cannot be obtained from the mold. Numerous mold materials and mold preparation methods can be used in the process of metal casting. Similarly, many core-making techniques are available. One of the more recent developments in mold and core-making has been the Croning shell mold process which was brought to the United States from Germany at the end of World War II.[2] Essentially, this process is the same for making molds and cores, therefore no distinction will be attempted when discussing the literature.

The shell molding process is unique in that it utilizes the thermosetting properties of synthetic resins to provide the bond between the sand grains in the construction of a mold. "Thermosetting is a term applied to resins (plastics) which solidify or set on heating and cannot be remelted. The thermosetting property usually is associated with a

cross linking reaction which forms a three-dimensional network of polymer molecules. In general thermoset materials cannot be reshaped once they have been cured."[3] Silica sand is used as the bulk refractory material for the majority of shell molds, however, other materials have received an increasing amount of attention in spite of higher cost.

Although a variety of synthetic resins[4-7] have been used in the foundry industry, most of these resins have been used for core-making in the presence of other binder materials such as clay, water, cereal, oil, gelatin, etc. These range from thermosetting to the newer self-curing or cold-curing resins. This application of resins should not be confused with the shell mold process. The two-stage phenol-formaldehyde resins remain the most popular for shell molding.

The problem of combining resin and sand has received some attention. Albanese[8] reports that although the original Croning process described the use of powdered resin intimately mixed with sand, methods that involve precoating of the sand with resin have given a more desirable product. Albanese further reports that the basic material for coating sand is the phenolic novolak resin.

Resin contents vary from 3% to 8% by weight. Capehart[9] has outlined the methods of coating sand according to the form of the novolak resin and the temperature at which the coating operation occurs.

Clifford,[10] Valyi,[11] and Gould[12] have discussed the two-stage resins used in shell molding. The two-stage resin is not a single material, but a mixture of phenol-formaldehyde (novolak) and hexamethylenetetramine (hexa). The novolak resin is thermoplastic due to a deficiency in formaldehyde and requires the addition of some form of formaldehyde before it will convert to the thermosetting stage. Under the influence of heat the hexa included in the sand-resin mixture will decompose releasing the necessary formaldehyde and ammonia which acts as a catalyst to make the novolak plus hexa mixture thermosetting.

Conventionally, the heat required for curing the resin bond has been supplied by placing the sand plus resin mixture in contact with heated (350 - 450°F) metal patterns. Conduction of the heat of the pattern into the mix will set or cure the resin binder to a thickness depending on the dwell time or time in contact with the heated pattern. The "shell" thus formed will conform to the dimensions of the

pattern. Wright[13] has developed a new method for providing the necessary heat to cure the resin. Specifically his process involves the addition of powdered susceptors to the mold mix, thus enabling him to cure the mold by use of induction heating. Iron, magnetite, and ferrosilicon powders were used by Wright to demonstrate the application of this process. Powder sizes of 100, 200, 325, and -325 mesh (Tyler series) and a 10KW, high frequency (400 kilocycles) induction unit were used in the above work. This method of curing eliminates the need for expensive metal patterns.

A survey of foundries using shell molding taken by a committee of the American Foundrymen's Society[14] in 1958 gave, among others, the following results. Shell thickness ranged from 1/8" to 1/2" with the majority of castings made in these shell molds being under 10#. Casting tolerances reported varied from ± .005" to ± .015" per inch. Gray iron, malleable iron, steel, stainless steel, magnesium, aluminum, brass, bronze, and special alloys were all being cast successfully in shell molds. Mold cracking and surface defects were listed as the most prevalent reasons for scrapped castings. The major advantages which have been claimed for shell molding include:[15,16]

1. Ability of the process to be highly mechanized.
2. Excellent surface finish is possible.
3. Good dimensional control is obtained.
4. Reduction of machining and finishing is inherited from advantages two and three.
5. Castings can be made of any of the commonly cast metals.

B. Surface Defects

It is necessary to become familiar with the changes which occur in the mold materials at casting temperatures because these changes are often responsible for surface quality problems. Apparently, the conditions existing when casting low carbon steels, where higher temperatures are involved represents the most severe occurrence of surface defects.

Certain forms of silica exhibit large expansion upon heating as shown in Figure 1[17]. Silica sand aggregates are usually quartz, but at higher temperatures the quartz may go through a crystalline inversion to cristobalite. In either case, the heating of silica sand will result in considerable expansion in the form of individual grain enlargement.

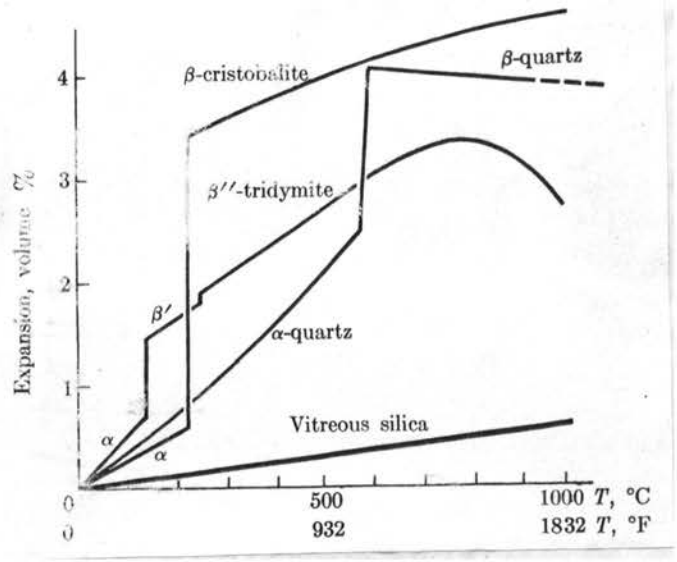

Figure 1. Thermal Expansion of Silica.[17]

This property of silica has been the source of undesirable distortion, buckling, spalling, and cracking of shell molds when subjected to elevated temperatures during casting. Cowles[18,19] investigated this thermal expansion problem and established the importance of aggregate selection. Shell molds were made of rounded, subangular, and angular silica sand (quartz) grains. Castings made in shell molds containing round sand grains had the most severe mold expansion. As expected, shell molds made with carbon sand and fused silica, which do not undergo such exaggerated expansion as regular silica sand, did not yield castings with surface defects due to sand expansion. Cowles then found that blends of 20% - 40% of the carbon sand or fused silica sand with the quartz sand gave thermal stability to the shell. Furthermore, shells made from bank sand (containing clay) gave improved casting surfaces. Rabe[20] also noted a decrease in surface defects due to mold expansion with bank sand shells compared to regular silica sand shells. Cowles explained the effect of the carbon sand, fused silica sand, and the clay in the bank sand as allowing "freedom of aggregate movement." In other words these additives provide a cushioning effect for the expanding silica.

Cowles[21] described the mechanism of expansion from the results of a test designed to study the expansion characteristics of hot shell molds. This test applies heat to one side of a specimen while loading the specimen transversely. Results showed that the initial movement occurred towards the heat application although loading opposed this movement. The heat conductivity through the sand and resin bond structure was slow enough to cause selective expansion of the grains first subjected to high temperatures, then deformation occurred with loading as the specimen reached uniform temperature at which time the resin binder is weakened.

The resins used as the binder are composed of a one to one molecular ratio of phenol, C_6H_5COH, and formaldehyde, CH_2O. Salzberg and Greaves[22] state that the cured phenolic resins contain an approximate composition of 80% carbon, 6% hydrogen, and 14% oxygen, and that the complicated reactions which occur in the combustion of this bond material during pouring depend primarily upon the availability of oxygen. After studying the properties of organic binders for steel molding sand, the Steel Founder's Society[23] reported that one of the chief disadvantages of resin binders is the enormous quantities of

gas released quickly as the resin is dissociated by heat into hydrogen, methane, carbon dioxide, nitrogen (from the hexa), and water vapor.

Thieme[24] determined that 80% - 90% of the gas evolved at 2500°F from a five-gram sand plus resin sample was released during the first 20 seconds, with most of the 80% - 90% being released between the sixth and twelfth seconds after combustion had begun. He further explains how the charring of the resin results in large volumes of gas being released with the carbon remaining between sand grains because of the deficiency of oxygen in the mold atmosphere needed for carbon combustion. This carbon can clog pores between sand grains resulting in decreased permeability.

Behring and Heine[25] discuss the carburization of the surface of steel castings which they attribute to the deposition of carbon film on the sand grains which is picked up by the molten steel during pouring. The carburized skin was discontinuous and non-uniform, being absent in some areas and quite thick in other areas. James and Middleton[26] investigated carbon pickup on the surface of steel castings in an attempt to relate carburization to surface defects. They found the surface carburization was

a somewhat erratic effect and was not associated with surface defects. James and Middleton did observe that additions of MnO_2, Na_2O, Na_2CO_3 or $CaCO_3$ in small percentages appeared to reduce carburization.

After close inspection of low carbon steel castings made in shell molds revealed a major defect which had the appearance of a surface blow, a program of research was sponsored by the Steel Founder's Society[27]. This research was guided by a theory developed to explain the cause of this defect on shell molded castings. This theory postulated that a time relationship between gas evolved and metal skin formation was such that the skin froze in a deformed state under pressure of the gas.

Results of this investigation showed the significance of several variables. Increased resin content in the shell molds increased the occurrence of the defect. Rapid pouring rate appeared to be a very beneficial condition for good surface detail. It was also observed that the surface defects were more pronounced in those parts of the casting where less ferro-static pressure was exerted. Shell molds having higher permeability at room temperature gave a slight improvement in the severity of the defect. Several granulated refractories were tested in place of

silica sand as the bulk material in shell molds. This resulted in the conclusion that zircon sand and forsterite shells produced excellent casting surfaces.

The final phase of this investigation was concerned with the effect of chemical additives to the shell molding mixture. Manganese dioxide (MnO_2) and ferric oxide (Fe_2O_3), when added to molding mixtures produced a decrease in the occurrence of surface defects. Five percent Fe_2O_3 was required for results equivalent to those obtained with 2% MnO_2. Other oxidizing agents were tested as additives and lead oxide (PbO_2) was found to be helpful as an additive to shell mixtures, primarily as an additive with MnO_2. Additions of calcium carbonate ($CaCO_3$) to shell mixtures were studied and found to be effective in preventing the formation of surface defects. The results were comparable to those obtained with manganese dioxide in correcting the surface defect.

Many other investigators[28-30] have made shell molds using olivine (commercial forsterite) and zircon for comparison with those made of silica sand shell molds. In all cases these materials gave a more satisfactory surface to low carbon steel castings. This improved surface has been attributed to the greater chilling ability of these

refractories which would facilitate the formation of a more stable skin.

Navarro and Taylor[31] performed extensive research on the effect of chemical additives to shell molding mixtures in an attempt to explain results previously reported - initially they found that cheaper grades of MnO_2 were not effective in preventing the surface defects. This suggested that MnO_2 might have a catalytic effect on resin decomposition, besides an oxidizing effect, the former being suppressed in the less pure grades. The fact that the addition of some very strong oxidizers did not improve the surface finish, while other inert oxides did improve the surface, reinforced the theory that the improvement gained with several chemicals is due mainly to their catalytic effect. Navarro and Taylor realized a marked improvement in casting surfaces with additions of carbonates, especially sodium, magnesium and calcium carbonates, however, results indicated a complex mechanism was responsible for the improvement and no complete explanation was given.

Powell and Taylor[30] also explained the effect of MnO_2 and $CaCO_3$. It was determined that both MnO_2 and $CaCO_3$ advanced gas evolution from the resin binder. The function

of the MnO_2 was that of oxidation producing a more rapid breakdown of the resin structure. The chilling effect of $CaCO_3$ was proposed to be related to its endothermic decomposition and the further endothermic reaction of CO_2 with carbon from the resin binder.

$$CaCO_3 \longrightarrow CaO + CO_2$$

$$CO_2 + C \longrightarrow 2CO$$

Powell and Taylor[32] used the beneficial chilling effect of the dissociation of $CaCO_3$ to develop the chillmet process which incorporates a composite, laminated mold. A facing layer of resin bonded refractory material is backed with carbonate - silica - resin mixture. This process eliminated defects associated with the reaction between molten steel and limestone.

C. Reactions between Iron Oxide and Silica

Iron oxide, usually in amounts under 5%, is a common additive to foundry sands, particularly in core sands. Riggan[33] first noticed the great improvement in the hot strength when core mixtures contained iron oxide. He used up to 5% Fe_2O_3 (approximately 200 mesh) and discovered an increase in the hot strength with increasing amounts of Fe_2O_3. Although Riggan offerred no explanation for the

improvement, Dietert[34] associated the increase in hot strength with the iron silicate formed at elevated temperatures when iron oxide is added to a core mixture.

Metal penetration was thought to be entirely of a mechanical nature until Dietert, Doelman, and Bennett[34] presented evidence of "oxide penetration". This mechanism occurs when iron oxide forms and fluxes the silica forming an iron silicate. Analysis of the burned-on layer of steel castings show it to be composed of Fe, FeO, Fe_3O_4, Fe_2O_3, iron silicate and SiO_2. Dietert et al, determined the effect of mold atmospheres on the interfacial reaction by casting steel pins in a cylindrical sand mold under various atmospheres. The interfacial reaction was absent under reducing conditions.

Darken[35] demonstrated that the temperature of fusion of iron oxides in contact with silica is a rather sensitive function of gas composition. A silica rod coated with Fe_2O_3 was placed in a furnace for heating under different atmospheres. With the aid of this data, Darken constructed a large part of the diagram showing the stable phases under various conditions of temperature and gas composition for the ternary system Fe-Si-O. This diagram is shown in Figure 2.

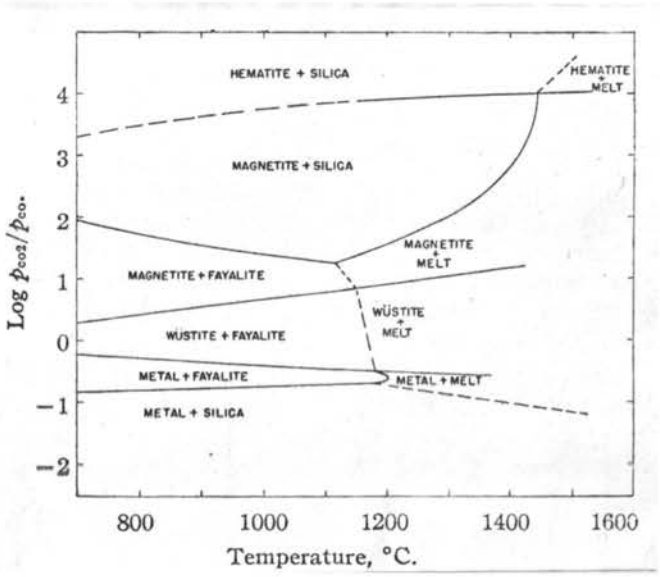

Figure 2. Stable phases of the system Fe-Si-O as a function of temperature and atmosphere.(35)

An extensive investigation of the interface reaction when steel is poured into sand molds was made by Savage and Taylor.[36] Samples of the sinter layer from production castings were compared to the reaction products obtained in the laboratory by induction melting a steel pin embedded in a sand specimen. Fayalite, $2FeO\ SiO_2$, was identified by X-ray diffraction analysis to be the only product formed by the interface reaction. This was found to be true of both production and laboratory samples. Because the mold and interstices between the sand grains are filled with air (21% oxygen), Savage & Taylor explain that "the fayalite was formed by oxidation of the iron of the steel and by subsequent reactions of the oxide with the silica sand". (For the sake of completeness, equilibrium diagrams of the system $Fe\text{-}Fe_2O_3$ and $FeO\text{-}SiO_2$ are included in Figures 3 and 4).

The Savage & Taylor investigation also included the effects of mold atmosphere and elements dissolved in the steel on the interface reaction. No reaction occurred in hydrogen or inert (nitrogen) atmospheres because there was no oxidation of the iron. Elements present in the steel which were more easily oxidized than iron were observed to retard the formation of fayalite because they decreased the

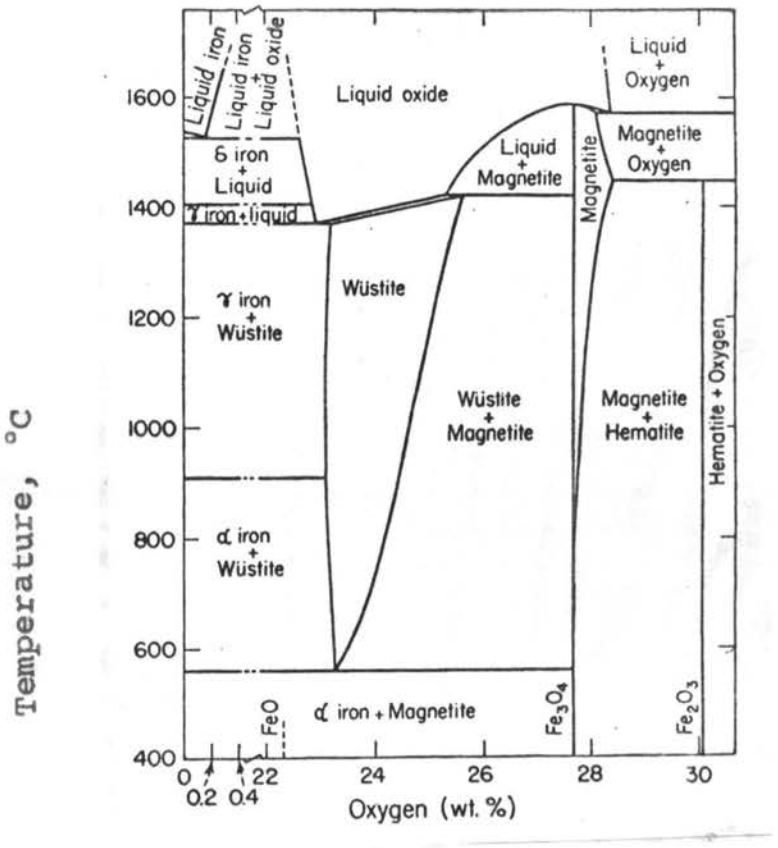

Figure 3. Equilibrium diagram of the system $Fe-Fe_2O_3$.(37)

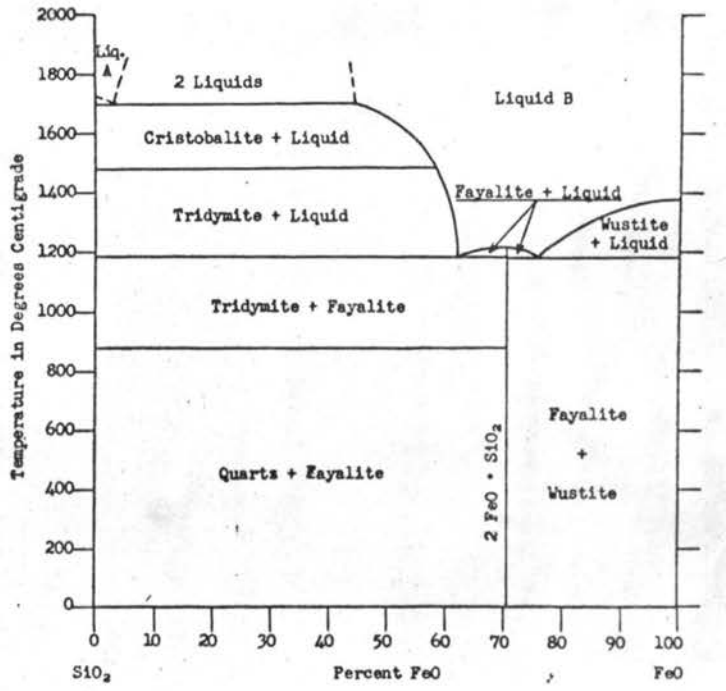

Figure 4. Equilibrium diagram of the system FeO-SiO_2.(36)

amount of oxygen available for the oxidation of the iron.

Colligan, Van Vlack, and Flinn have also studied the iron-silica interface reaction.[38] Preliminary results of their study agree with those of Savage & Taylor previously discussed, i.e., iron oxide is formed which dissolves the silica to form an iron silicate melt which crystallizes to fayalite on cooling. Colligan and coworkers did expand the theory of fayalite formation to include reactions occurring at temperatures (1225° - 2237°F) well below the melting point of iron. Iron powder and quartz grains were heated in a globar furnace under various combinations of temperature and gas compositions (CO_2/CO ratios). Results showed that below a critical CO_2/CO ratio, which depends on temperature, no mold attack occurred. Increased temperatures resulted in a more pronounced attack. In a separate investigation[39], these same investigators compared the interface reaction in green sand molds and shell molds. The atmosphere produced by phenolic resin bonded shell molds resulted in very slight reaction. The effect of an oxidizing mold atmosphere was demonstrated in the green sand castings by extensive reaction at the interface. Colligan, et. al. conclude that the reducing nature of the shell molds prohibits interface reactions.

III EXPERIMENTAL PROCEDURE

It will be advantageous if the procedures followed in the individual phases of this investigation are discussed separately. Therefore, the discussion of the experimental procedure is subdivided into three phases:

A. Preparation of Mold Materials

B. Making of Molds

C. Pouring and Analysis of Castings

A. Preparation of Mold Materials

Sands of the refractory oxides, silica - SiO_2, and zircon - $ZrO_2 \cdot SiO_2$ were used as the bulk material for the molds. Washed and dried sands (rounded grains) were used. These sands contain negligible clay content. The sands used in this study are comparable to those recommended by the American Foundrymen's Society for use in shell molding.[40] A third substance, crushed magnetite (angular particles), Fe_3O_4, containing less than 5% impurities was selected to be used as an additive to the bulk materials. This addition of Fe_3O_4 constitutes the foundation of this investigation.

A screen analysis performed on the silica and zircon

sands gave an AFS grain fineness number of 105 for the silica sand and 152 for the zircon sand. Calculations of the AFS fineness number and graphs showing the size distribution in both of these sands are contained in Appendix I.

Although sand precoated with resin is commercially available, it was felt a greater degree of control resulting in more uniformity would be obtained by coating the mold materials in the laboratory. A two-stage phenolic resin was used. Each of the substances, silica sand, zircon sand and crushed magnetite were coated separately. Coating procedure followed that recommended by the resin manufacturer[41], the typical procedure being outlined below:

1. Weigh 4.75 kilograms of silica sand.
2. Add 30 grams powdered hexamethylenetetramine (hexa).
3. Add 2.5 grams powdered stearate wax.
4. Place above in clean Simpson laboratory muller and mull for two minutes.
5. Add 250 grams liquid novolak resin (70% solids).
6. Mull for 15 minutes making a second wax addition (2.5 grams) near the completion of the mulling

cycle.

7. Remove from muller and spread for drying.

The hexa serves as a catalyst and the wax is included to improve flow characteristics and as a release agent. Both the hexa and wax are added as a percent of the liquid resin, 12% and 4% respectively.

The percent resin in the above coated sand can be calculated as 5.3%.

$$\% \text{ Resin} = \frac{\text{weight resin}}{\text{total weight}} (100)$$

$$= \frac{(250 + 30 + 5) \text{ grams}}{(4{,}750 + 250 + 30 + 5) \text{ grams}} (100)$$

$$= \frac{285}{535} (100) = 5.3$$

To get an equivalent volume percent of resin on the zircon and magnetite, the densities must be considered. In this investigation the zircon was coated with 3% resin, which is equal in volume percent to 5.3% resin in silica sand. No compensation for the density of magnetite was made and, therefore, it was coated with 5.3% resin by weight. However, it should be mentioned that the magnetite was difficult to coat and resin losses during coating are of possible significance. Additional information concerning the resin

content of the coated magnetite is offerred in later discussion (Appendix II). Below is a table of mold materials, densities and weight percent of resin with which the respective materials were coated.

Material	Density	Weight % Resin
Silica Sand	2.65	5.3%
Zircon Sand	4.56	3.0%
Magnetite	5.18	5.3%

Coated silica and zircon sands were passed through a 48 mesh (Tyler series-screen opening .0116 inches) screen to remove the coarse material. After coating, the magnetite was separated by mechanical screening equipment into the following sizes:

Mesh Number (Tyler)	Screen Opening (inches)	Average Diameter of Particle Retained (42) (inches)
48	.0116	Discarded
65	.0082	.0099
100	.0058	.0070
150	.0041	.0050
200	.0029	.0035
325	.0017	.0022
-325	No subsieve analysis was made	

This completed the preparation of the mold materials which are to be used to provide the various mold mixtures in this study. After screening of the magnetite, some tests were made in an attempt to determine the variation in resin content with particle size. This procedure and the results are included in the Appendix II.

B. Making of Molds

Since this investigation is primarily concerned with conditions at the mold-metal interface, the mold cavity which is to be filled with molten metal must be of suitable design to allow an evaluation of these conditions on the final casting. With this in mind the casting shape and feeding arrangement shown in Figures 5 and 6 were developed for this study. This design incorporates a bottom pour system which minimizes pouring defects. Metal will be poured into a pouring cup, then flow down the tapered sprue into the runner and finally enter the mold cavity through a choked ingate.

Section BB in Figure 6 shows the cross section of the casting to be used in studying the mold-metal interfacial conditions. Various cooling rates are inherent in the wedge shaped casting. Each side of the wedge contains a sufficient area to allow representative interfacial

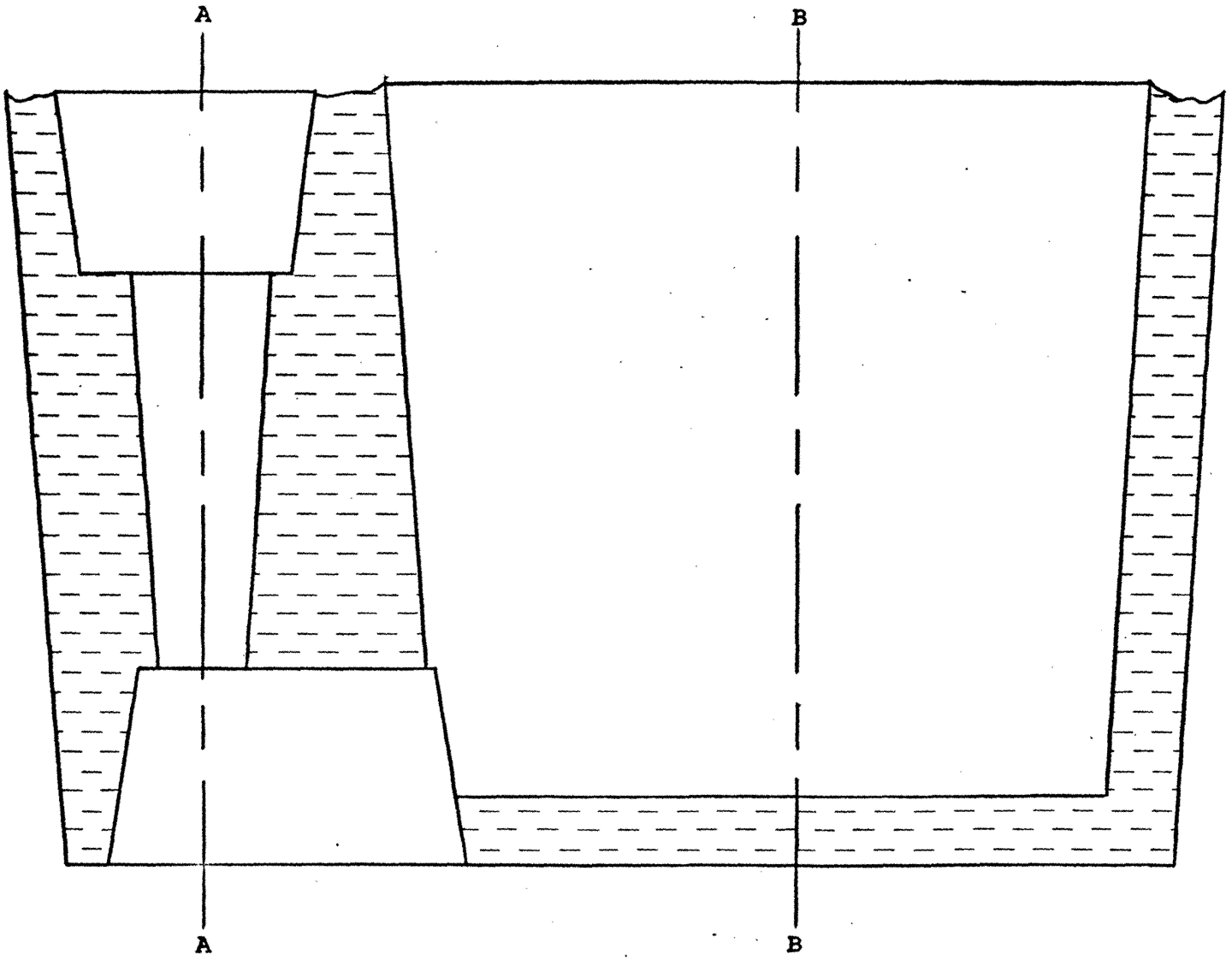

Figure 5. Longitudinal section of mold (actual size).

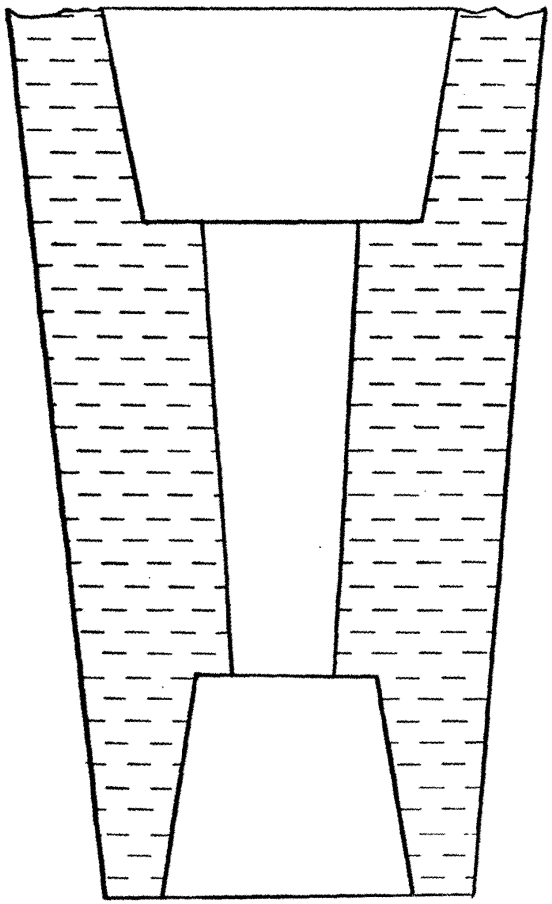

Section AA

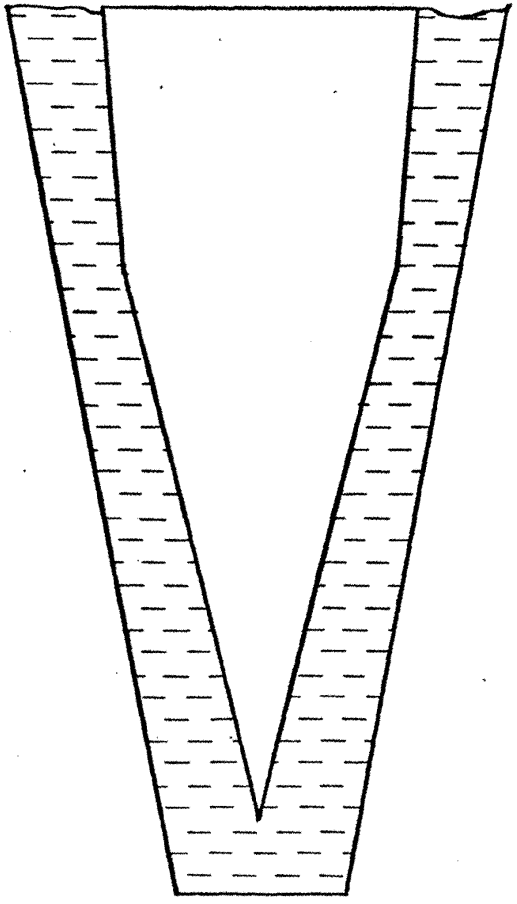

Section BB

Figure 6. Transverse sections of mold (actual size).

conditions to develop.

Once the design described above was determined, the next step was to make a pattern to form a cavity of the desired shape and a mold box to form the outside surface of the mold. A three-part pattern was used as shown in Figure 7. Transite and wood were used as pattern material. The mold box was made from wood and masonite. Positioning of the patterns and addition of the mold material in preparation for the making of a mold was accomplished as follows:

1. The pattern for the runner was permanently attached to the bottom of the mold box.
2. The pouring cup and sprue assembly was positioned on the runner by a dowel pin on the latter which fit into a hole in the base of the sprue.
3. A layer (approximately 1 inch thick) of mold material was placed on the bottom of the mold box.
4. The main pattern of the casting to be studied, was put in the mold-box using the matching surfaces between it and the runner pattern for allignment.
5. The remaining space, as can be seen in Figures 5 and 6, was filled with mold material.

Figure 7. Photograph of three part pattern used to form mold cavity.

Various compositions were used as the mold material. The majority of the mixes had a silica sand base to which the magnetite of a specific particle size was added in weight percentages ranging from 10% to 50%. A few mixes of zircon sand plus magnetite were made. The different mold materials were thoroughly mixed before using. For comparative purposes, some mold mixes contained no magnetite; they consisted of silica sand or zircon sand. A table describing the composition of each mold is contained in Appendix III.

Curing of the molds was done by the use of induction heating. The magnetite particles served as the susceptor material in the mold mix. For those mixes which contained no magnetite, an aluminum pattern was used to cure the mold material. These no-magnetite mixes were only used around the pattern which represented the casting to be studied. Regular mixes containing magnetite were used in the remainder of the mold.

Because of the shape of the mold, it was necessary to make an induction coil of similar shape to obtain uniform heating. This coil was made by wrapping 50 feet of 1/4 inch O.D. copper tubing around a form and then spacing each turn of the coil on 1/2 inch centers. The coil contained

24 turns making it 12 inches in length. Wooden pieces were used on the top and bottom of the coil to determine the spacing and make the coil rigid. The bottom piece also provided a platform which enabled the mold to travel through the coil during curing. This coil was used with a 10 KW, 400 KC Lepel induction unit.

When a mold was assembled for curing it was placed in the coil and the power was turned on. The system for pulling the mold through the coil consisted of a nylon string attached to the mold box and connected to a chain which was engaged by a gear mounted on the shaft of a variable speed motor. The molds were not pulled at a constant speed through the coil because this failed to give a uniform cure. Instead, through experience the relative rates of cure in the various areas of the mold were determined and the cycle for pulling the mold through the coil was manually adjusted accordingly. Curing times ranged from five minutes to 1 hour and 15 minutes depending on the size and amount of magnetite in the mold material. When the aluminum pattern was utilized, curing times were approximately thirty minutes. Photographs of the experimental apparatus are included in Figure 8.

When the molds were observed to be sufficiently cured, they were removed from the coil. Since they were hot,

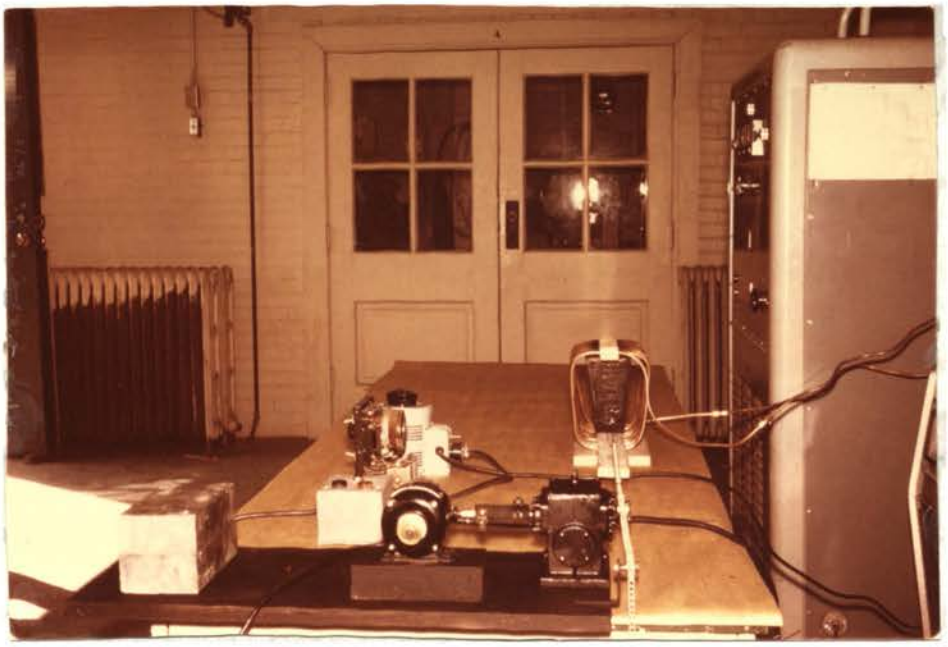

Figure 8. Photographs of experimental apparatus. Note mold being cured in coil.

they were handled with asbestos gloves. The main pattern was withdrawn with pliers. The mold box was then inverted and rapped until the mold dropped from it. Since the runner pattern was attached to the mold box, it was also removed in this operation. This left the base of the sprue pattern exposed, thus allowing the removal of the remaining pattern by lightly tapping this base. An identification number was placed on each mold with hot marking crayon. Representative pictures of the finished molds are shown in Figures 9 and 10.

C. Pouring and Analysis of Castings

All molds were taken to a commercial foundry, Oklahoma Steel Castings of Tulsa, Oklahoma, for pouring. In preparation for pouring, each mold was blown out with compressed air and placed on a firebrick embedded in green sand as shown in Figure 11A. The firebrick served as the bottom surface of the runner. After placing a paper towel over the top of each mold to prevent dirt from entering the mold cavity, green sand was packed around the mold. The molds were transferred to the pouring area where the pouring basin was uncovered and another firebrick was placed over the mold cavity to guard against splash during pouring. A weight was placed on top of this firebrick to

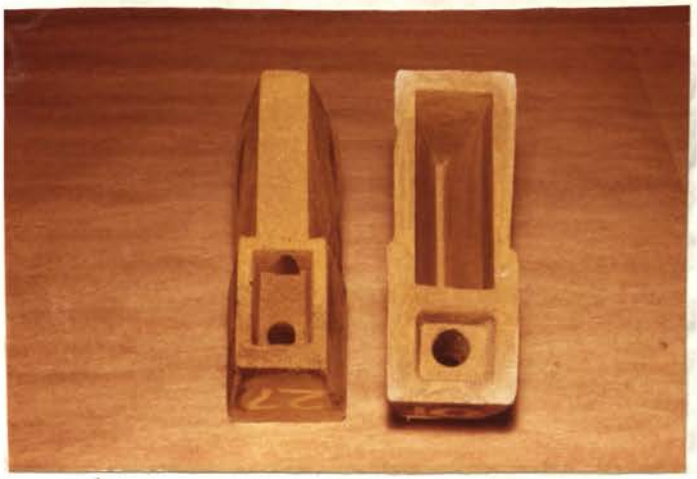

A. Top and bottom view of finished mold.

B. Segregation of magnetite in molds containing 50% +65 mesh magnetite (left) and 50% +100 mesh magnetite (right).

C. Composite molds made with aluminum pattern.

Figure 9. Representative photographs of finished molds.

A. Molds containing (left to right) 10, 20, 30, 40, and 50 percent +200 mesh magnetite.

B. Molds containing (left to right) 10% +65, 30% +200, and 50% +325 mesh magnetite.

Figure 10. Effect of composition on appearance of finished molds.

insure against any "floating" of the mold during pouring. The weight and brick were removed immediately after pouring. Pouring of the molds can be seen in Figure 11B.

The steel used for pouring the castings was obtained from a four ton heat melted in an electric arc furnace. The steel was deoxidized with aluminum additions to the ladle. Composition of the steel was as follows:

C.	Mn.	P.	S.	Si.
.26	.70	.032	.028	.52

Pouring temperatures ranged from 2950°F for the first molds poured to 2900°F for the last molds poured.

Following pouring the castings were moved from the pouring area and allowed to cool. Removal of the mold material from the casting represented no problem because the mold loses its strength when the resin binder burns out. Each casting was identified with the number of the mold into which it was poured. Samples of the sand adjacent to the mold-metal interface were collected and identified with its respective mold number. This completed the portion of this study performed with the cooperation of Oklahoma Steel Castings.

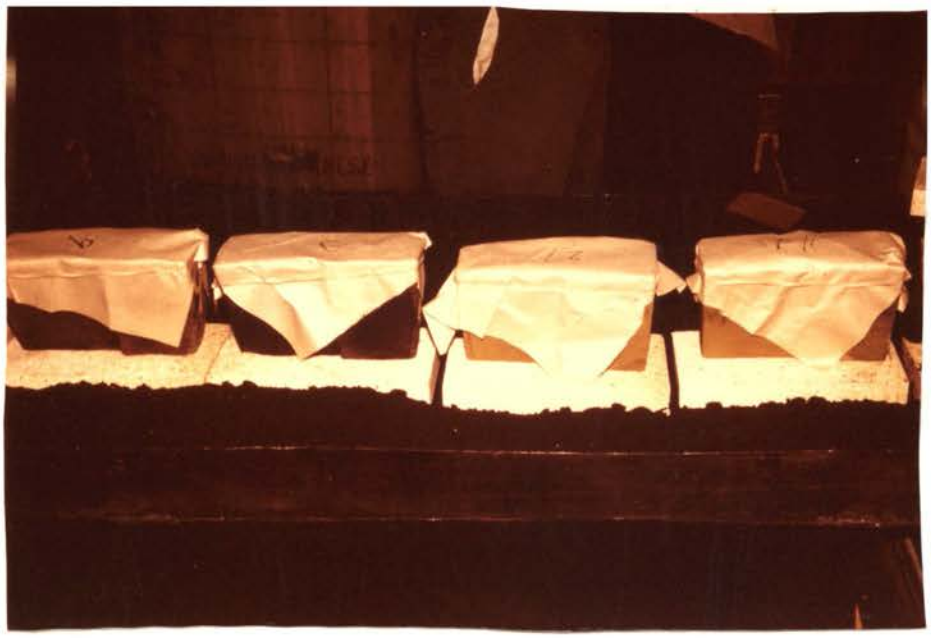

A. Molds placed on firebricks and covered for protection. Next green sand was heaped up around the molds.

B. Pouring of molds from 100# ladle.

Figure 11. Preparation for and pouring of molds.

Samples of the castings produced in this investigation can be seen in Figure 12. Runners and sprues were cut from the castings using a band-saw. Scale and small amounts of adhering mold material were removed from the casting surface by sand-blasting. This left the surface in an excellent condition for visual inspection. Photographs of the surfaces of each of the castings were taken. Several of the castings were then cut up for macro and micro examination.

Figure 12. Sample photographs of castings made for this investigation.

III RESULTS

A. Introduction

Representative surfaces of each casting produced in this investigation are shown in Figure 13 through Figure 21. These photographs are approximately 1/6 actual size and depict the entire surface of one side of the casting after removal of runners and sprues and after sand blasting. The photographs of the casting surfaces are presented in groups which were made in molds containing additions of magnetite of the same particle size, beginning with those made in molds with +65 mesh magnetite and proceeding to those made in molds containing -325 mesh magnetite (Figures 13 to 18). These are followed by castings produced in normal silica sand shell molds (Figure 19) and special shell molds (Figures 20 and 21). Each casting is identified by individual captions and by the main caption for the respective Figure.

Comprehension of the results will be facilitated by first distinguishing between the various surface defects or conditions which are readily observed in a comparison of casting surfaces. The most consistent surface condition, as shown in Figure 19, was found on the castings made in silica sand shell molds containing no magnetite.

These surfaces are caused by thermal expansion of the mold material. None of the castings produced in molds containing the magnetite additive show any indication of the expansion defect. However, many of these castings did exhibit poor surfaces due to one of two other defects or a combination of both. The first surface defect is characterized by small beads on the surface resulting in surface roughness to a degree dependent on the size, shape, and number of beads. Examples of this defect can be seen in Figure 13-B,D & E. The second defect exhibited by the molds containing magnetite appears as a surface blow, examples of which can be seen in Figure 18-C & D. Combinations of the two defects may also occur as shown in Figure 13-C. Although these undesired surfaces were predominate, many of the castings from molds containing magnetite had excellent surfaces (Figure 14-1-A & B).

A few castings, Figures 15-A, 16-1-F, show evidence of metal splash on the surface. Several other castings contain defects at the very bottom as a result of similar faulty pouring. These defects, as well as irregularities which occur in the extreme top of the casting, will not be considered in this investigation because they cannot be attributed to the mold material.

With the background obtained from the identification of the surface defects discussed above, it is unnecessary to treat the surface appearance of each casting individually. Instead the specifics of each defect or surface condition will be presented in detail.

B. Expansion Defect

As previously mentioned, the rough surface caused by the expansion of the mold material was eliminated by the use of the magnetite additive. The most conclusive casting in this respect is casting #41. This casting was made in a composite mold which had 30%, +200 mesh magnetite on the right side, but the left side of the mold contained no magnetite. Figure 20 shows the expansion defect occurred on the left side but not on the right.

The mechanism by which the expansion defect occurs is shown in Figure 22. Initially, a skin of solidified metal is formed which is thicker at the bottom because of the decreased cross section. As the sand expands, the wall of the mold will buckle outward in an effort to relieve the expansion stresses. Since the actual wall movement is small at the bottom, this area is unaffected (Zone 1). As the wall movement increases in Zone 2, the skin is pulled out by its adherence to the mold. However in Zone 3, the

skin is weak and does not adhere as strongly to the mold, therefore only selective areas of the skin are "punctured" which allows metal to escape to the final position of the mold wall.

Microscopic examination of the castings exhibiting the expansion defect revealed that the portion of the casting in intimate contact with the mold wall (shaded portions in Figure 22) were carburized. The photo-micrograph of Figure 23-A is a typical surface structure found in these areas. No carburization was discovered in the portion of the castings in Zone 3 which were not in contact with the mold as can be seen in Figure 23-B. Figure 23-C shows both the carburized and unaffected structure.

Samples taken from identical locations on opposite sides of casting #41 gave interesting results as shown in Figure 24. The location of the samples was approximately 1" from the bottom of the casting. The photomicrographs show carburization on the silica sand side but no indication of carburization on the side containing the magnetite addition. From the preceding paragraph, carburization of both of these surfaces would be expected because they would both be in contact with the mold.

Although the special shells made with zircon sand,

Figure 21, also produced castings which possessed a similar expansion defect, the defect was much less severe. Carburization of the surface was found to follow the same pattern as was found in the castings made in the silica shells.

C. Surface Beads

This condition is apparently related to the pickup of magnetite from the mold. The beads on the surface of the casting occurred both as smooth, rounded beads which appeared to be an integral part of the casting, and as sharp particles which appeared to be only stuck on the surface. Some of the larger beads were an agglomeration of smaller ones.

By comparing the casting surfaces shown in Figures 13 through 18, the severity of this defect is seen to increase with both magnetite particle size and percent magnetite. The size of the beads also increases with increasing magnetite particle size in the mold. Therefore, it is not surprising to find the worst occurrence of this type defect on the surfaces of the castings made in the molds containing 50%, +65 mesh magnetite (Figure 13-D & E). Likewise, it is not surprising to find the complete disappearance of this defect on castings from molds containing the small (+325, -325) magnetite particles regardless of the percentage.

The results of microexamination of sections through the castings which exhibited the beaded surface condition are contained in the photomicrographs of Figures 25 and 26. Referring to Figure 25, the contrasting surface structure of the two parts of the casting is easily observed. Within the bead, there are voids making it appear rather porous. Additional bead structures are included in Figure 26. These pores were found in all of the beads examined. Some of the beads contained several small pores (Figure 26-A & B) where others contained a single large pore (Figure 26-C). No correlation could be made between the size of the pores and the mold composition. It was possible to remove small particles from a few of the pores, however no identification of these particles was accomplished. Carburization was found to occur beneath most of the beads, but no carburization was discovered in other portions of the casting.

Zircon sand shells containing 30%, +150 mesh magnetite (Figure 21-C & D) showed no improvement over silica sand shells containing the same size and percentage of magnetite (Figure 15-C & D).

D. Surface Blow

Evidence of a gas blow on the casting surfaces ranges from light effects (Figure 26-1-C & D) to a very pronounced

condition (Figure 18-C & D). Although some traces of gas blows can be seen on the castings made in molds containing magnetite larger than +200 mesh, the detrimental effects of gas blows on surface quality are restricted to the castings produced from molds whose composition included magnetite of a particle size of +200 mesh or less. The only exception is casting #20, Figure 13-C, The severity of the surface blow condition increases with increasing percent magnetite and decreasing magnetite particle size. The defective surface resulting from the gas blow is concentrated in the upper portions of many of the castings. Molds of a composition of zircon sand and 30%, +200 mesh magnetite (Figure 21-E & F) gave castings with poor surfaces due to the gas blow defect. Silica sand molds made with the same size and percentage of magnetite produced castings with satisfactory surfaces (Figure 16-1-E & F).

Microexamination revealed very few areas of carburization. These carburized areas seemed to be concentrated under the pockets formed on the surface by the blow. An example of this carburization is shown in Figure 27-A. A dendritic structure is also apparent in Figure 27-A. This structure could be the result of a slower cooling rate due to insulation by the gas being given off by the

mold material. Emphasis is placed on the fact that a carburized surface was the exception and was not characteristic of the surface structure of this class of castings. A more representative structure is shown in Figure 27-B. This photomicrograph is also from an area beneath the surface defect caused by a gas blow.

E. Acceptable Surfaces

Several of the mold compositions used in this investigation did yield castings with high quality surfaces. The best castings were produced from molds containing 10%, +100 mesh magnetite as shown in Figure 14-1-A & B. Surface structures representative of those observed in the good castings are included in Figure 28.

F. Summary of Results

Expansion defects have been shown to occur on the castings of this study made in regular silica sand shell molds. Although additions of magnetite in the mold material eliminated this defect, two other surface defects occur when magnetite is present in the mold material. These are the surface beads, related to pickup of magnetite from the mold, and gas blows. Several castings made in the shell molds containing magnetite had acceptable surfaces.

A summary of the surface condition of the castings made in this investigation is contained in Appendix III. Although some of the castings which have been rated as acceptable may contain isolated defects, this rating represents an indication of promise for the respective shell mold composition from which these castings were produced. Primarily, it was the wedge portion of the casting which was judged. It should be remembered that all these castings were sand blasted, a process which will uncover the slightest surface irregularity.

The data contained in Appendix III are plotted in Figure 29. Only those molds composed of silica sand and magnetite have been plotted. In those cases where the casting was considered a borderline case, it is represented on the graph by both the accepted and rejected symbols.

Figure 29 illustrates the systematic occurrence of the surface defects observed in this investigation. Any combinations of size and amount of magnetite which fall to the left of line ABC resulted in surface blows, any combinations which fall to the right of line DEF resulted in surface beads. The area BCDE represents a transition zone between the two defects. The line ABEF represents

the perimeter of the combinations of size and amount of magnetite which gave a casting rated as acceptable. This is not intended to be interpreted to mean that any combination which falls within the area bounded by ABCD will always yield an excellent casting.

A. Casting #8
10% Magnetite (+65)

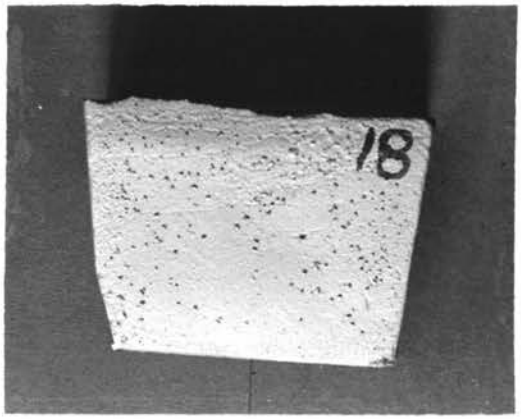

B. Casting #18
30% Magnetite (+65)

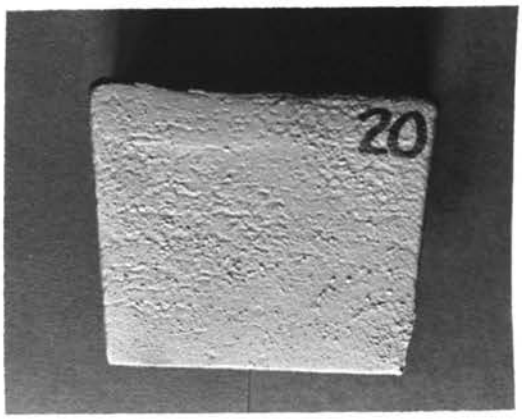

C. Casting #20
30% Magnetite (+65)

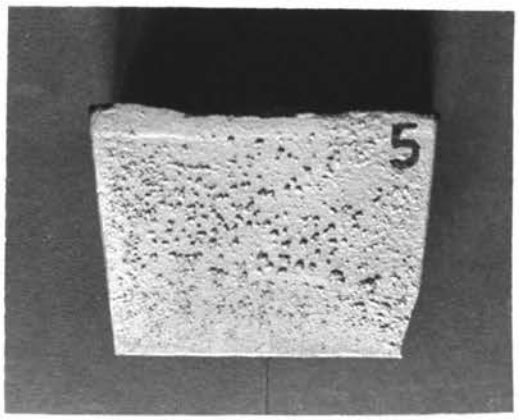

D. Casting #5
50% Magnetite (+65)

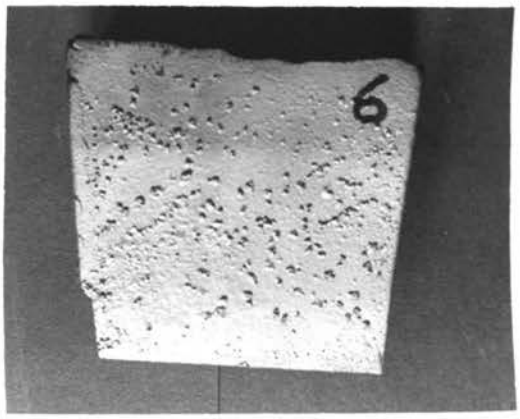

E. Casting #6
50% Magnetite (+65)

Figure 13. Photographs of surfaces of castings poured in molds containing silica sand and +65 mesh magnetite.

A. Casting #3
10% Magnetite (+100)

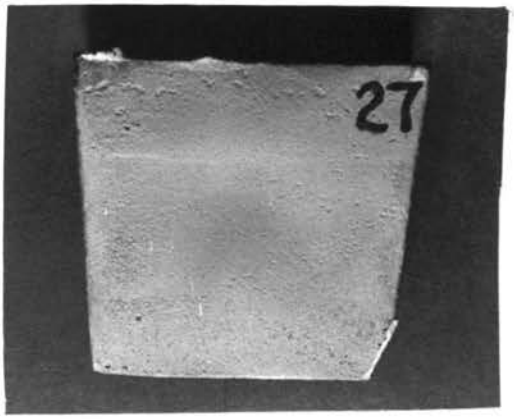

B. Casting #27
10% Magnetite (+100)

C. Casting #47
20% Magnetite (+100)

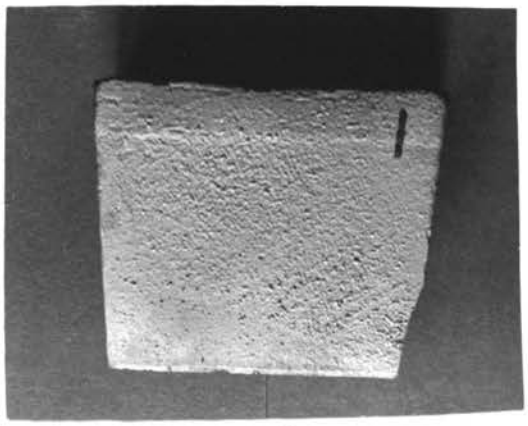

D. Casting #1
30% Magnetite (+100)

E. Casting #14
30% Magnetite (+100)

Figure 14-1. Photographs of surfaces of castings poured in molds containing silica sand and +100 mesh magnetite.

F. Casting #42
40% Magnetite (+100)

G. Casting #43
40% Magnetite (+100)

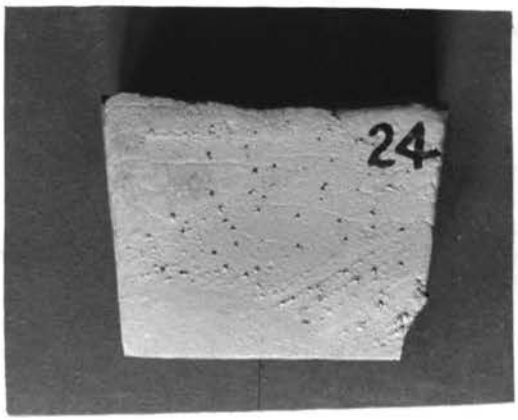

H. Casting #24
50% Magnetite (+100)

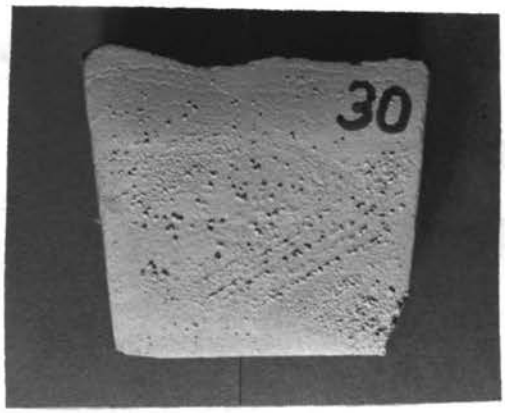

I. Casting #30
50% Magnetite (+100)

Figure 14-2. Photographs of surfaces of castings poured in molds containing silica sand and +100 mesh magnetite.

A. Casting #12
10% Magnetite (+150)

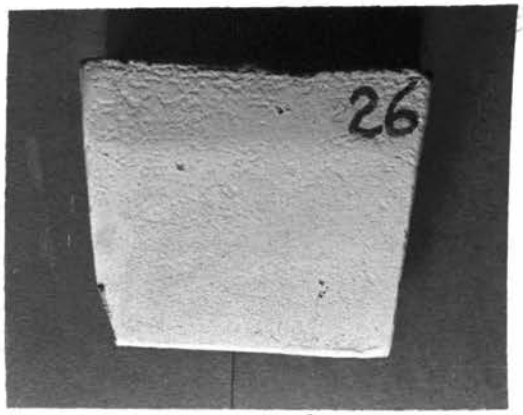

B. Casting #26
10% Magnetite (+150)

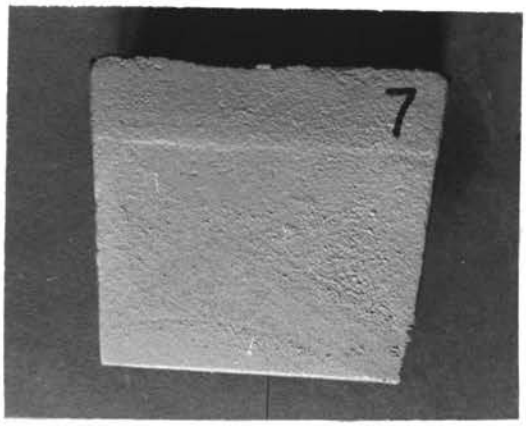

C. Casting #7
30% Magnetite (+150)

D. Casting #21
30% Magnetite (+150)

E. Casting #29
50% Magnetite (+150)

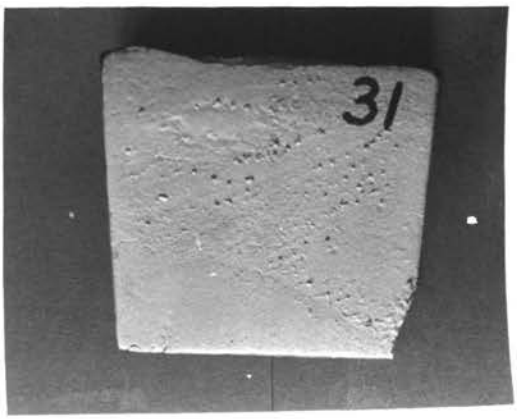

F. Casting #31
50% Magnetite (+150)

Figure 15. Photographs of surfaces of castings poured in molds containing silica sand and +150 mesh magnetite.

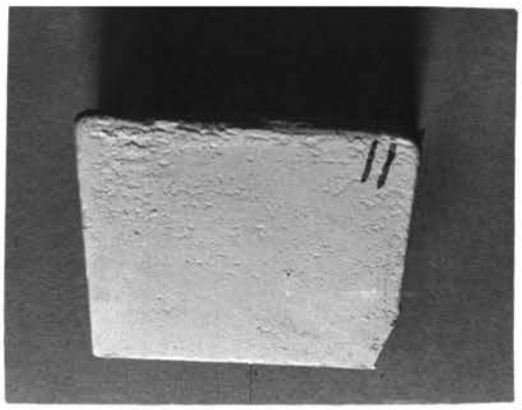

A. Casting #11
10% Magnetite (+200)

B. Casting #16
10% Magnetite (+200)

C. Casting #44
20% Magnetite (+200)

D. Casting #46
20% Magnetite (+200)

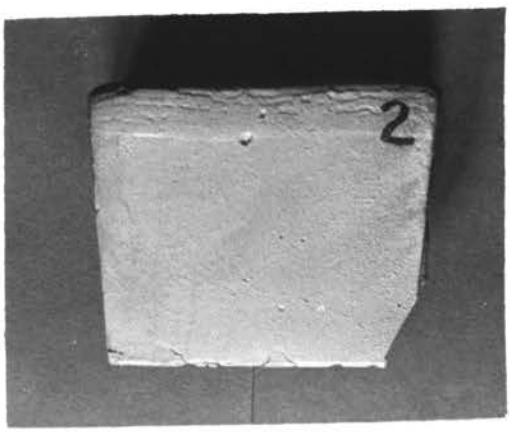

E. Casting #2
30% Magnetite (+200)

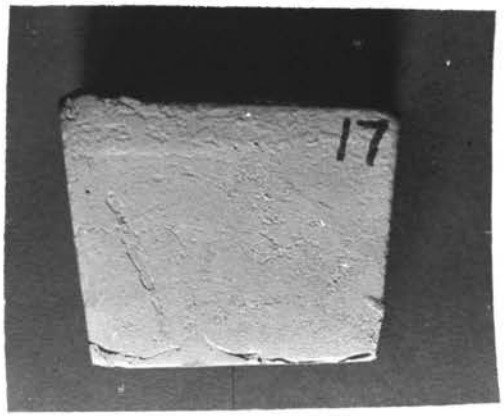

F. Casting #17
30% Magnetite (+200)

Figure 16-1. Photographs of surfaces of castings poured in molds containing silica sand and +200 mesh magnetite.

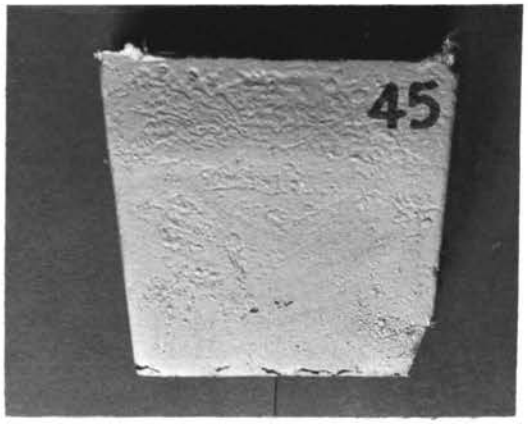

G. Casting #45
40% Magnetite (+200)

H. Casting #48
40% Magnetite (+200)

I. Casting #25
50% Magnetite (+200)

J. Casting #28
50% Magnetite (+200)

Figure 16-2. Photographs of surfaces of castings poured in molds containing silica sand and +200 mesh magnetite.

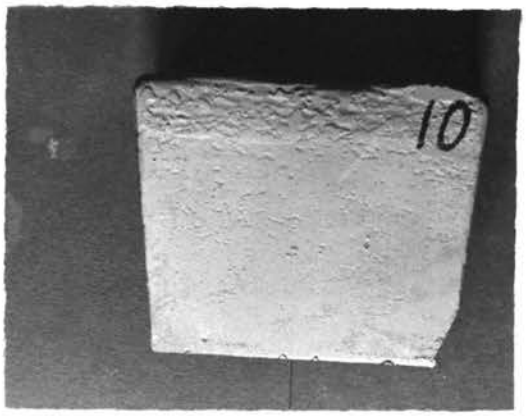

A. Casting #10
10% Magnetite (+325)

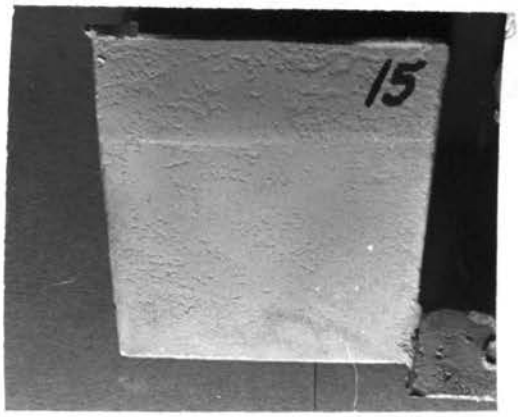

B. Casting #15
10% Magnetite (+325)

C. Casting #13
30% Magnetite (+325)

D. Casting #22
30% Magnetite (+325)

E. Casting #32
50% Magnetite (+325)

F. Casting #34
50% Magnetite (+325)

Figure 17. Photographs of surfaces of castings poured in molds containing silica sand and +325 mesh magnetite.

A. Casting #9
10% Magnetite (-325)

B. Casting #19
10% Magnetite (-325)

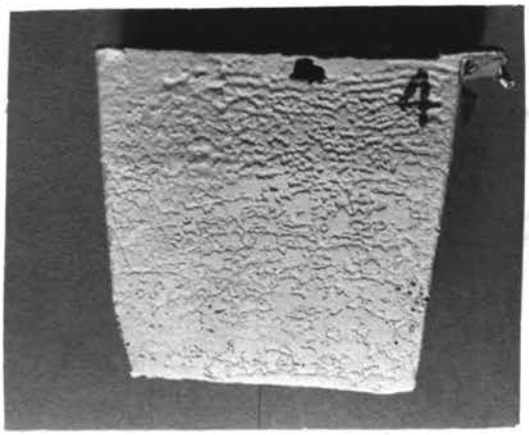

C. Casting #4
30% Magnetite (-325)

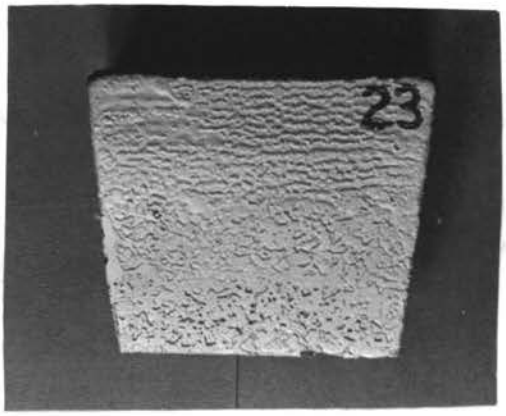

D. Casting #23
30% Magnetite (-325)

Figure 18. Photographs of surfaces of castings poured in molds containing silica sand and -325 mesh magnetite.

A. Casting #35
Silica Sand

B. Casting #36
Silica Sand

B. Casting #37
Silica Sand

C. Casting #38
Silica Sand

D. Casting #39
Silica Sand

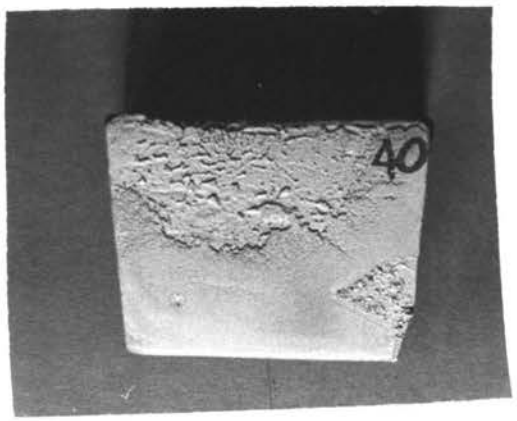

E. Casting #40
Silica Sand

Figure 19. Photographs of surfaces of castings poured in regular silica sand shell molds.

A. Casting #41 (Right Side)
Silica Sand
30% Magnetite (+200)

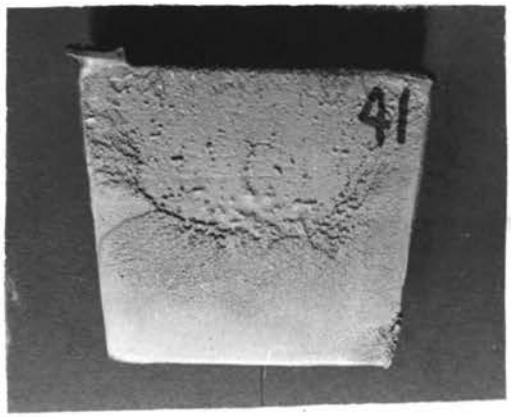

B. Casting #41 (Left Side)
Silica Sand

Figure 20. Photographs of both surfaces of casting #41 made in composite mold.

A. Casting #49
Zircon Sand

B. Casting #50
Zircon Sand

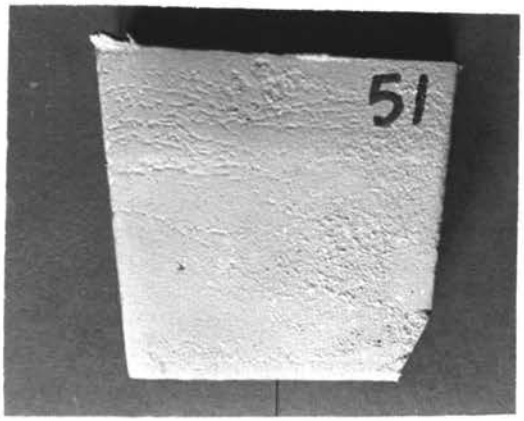

C. Casting #51
30% Magnetite (+150)

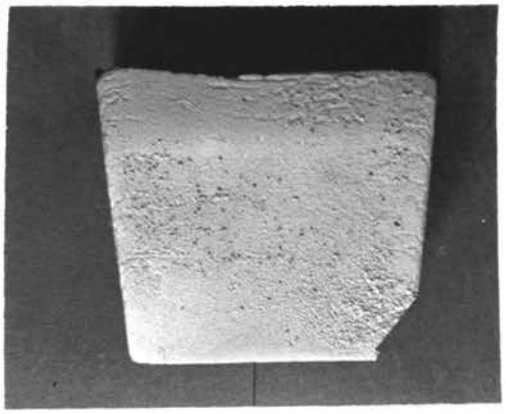

D. Casting #52
30% Magnetite (+150)

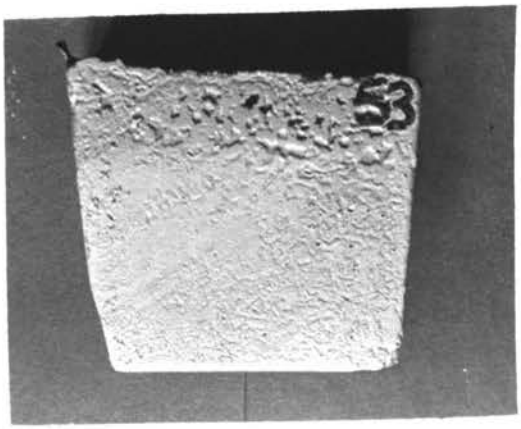

E. Casting #53
30% Magnetite (+200)

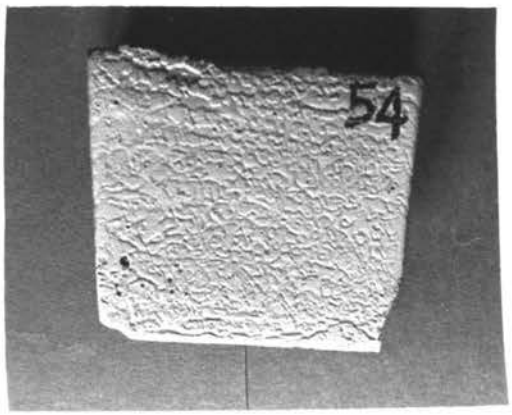

F. Casting #54
30% Magnetite (+200)

Figure 21. Photographs of surfaces of castings poured in molds containing zircon sand or zircon sand plus magnetite.

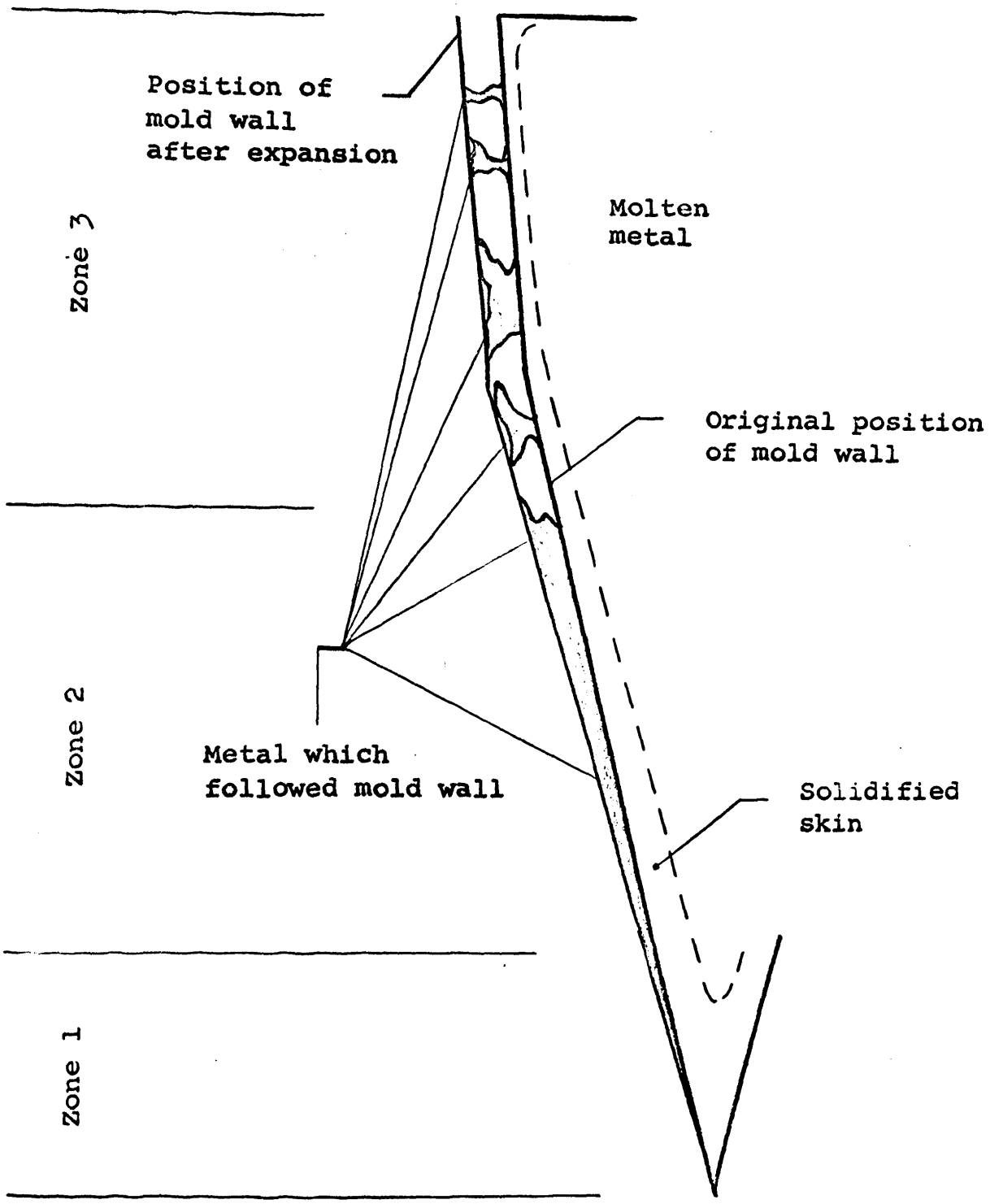

Figure 22. Schematic representation of rough surface due to mold material expansion.

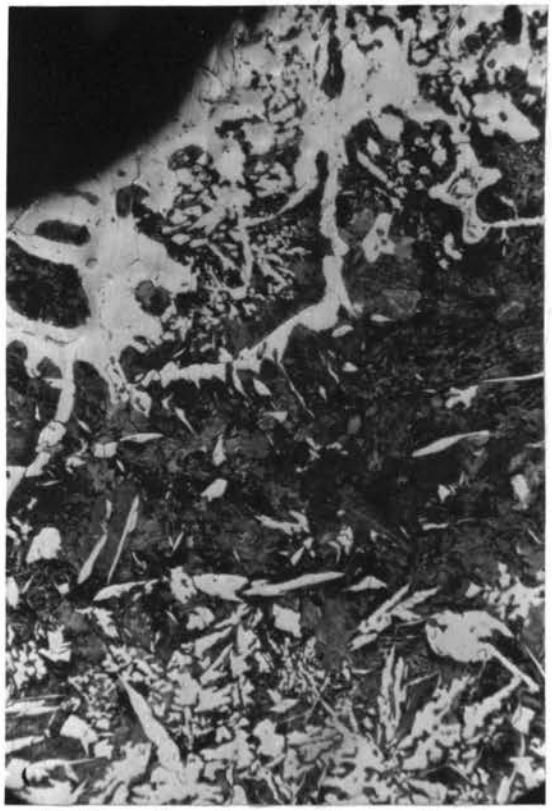

A. Carburized surface from zone 3 which was in contact with mold wall after expansion.

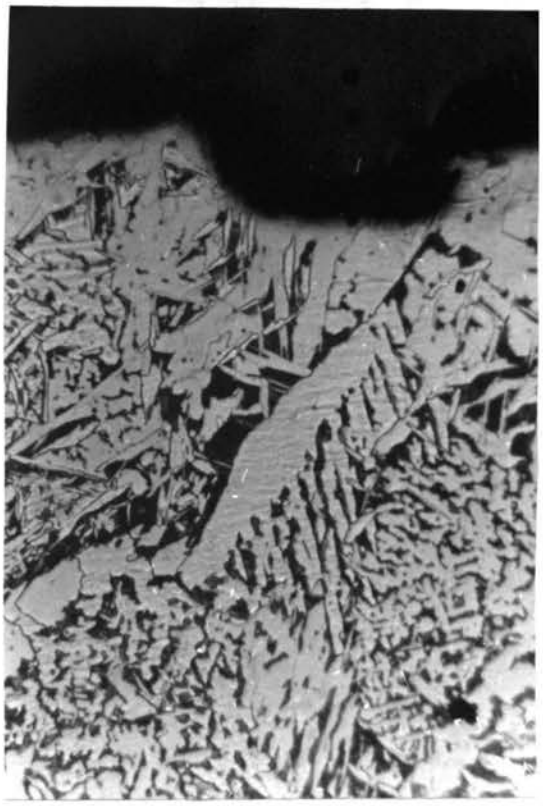

B. Uncarburized surface from zone 3 which was not in contact with mold wall after expansion.

C. Transition area from carburized (left) to uncarburized (right) surface.

Figure 23. Photomicrographs (100X) from casting #37 representative of the surface structure of castings exhibiting expansion defects. Etchant 5% Nital.

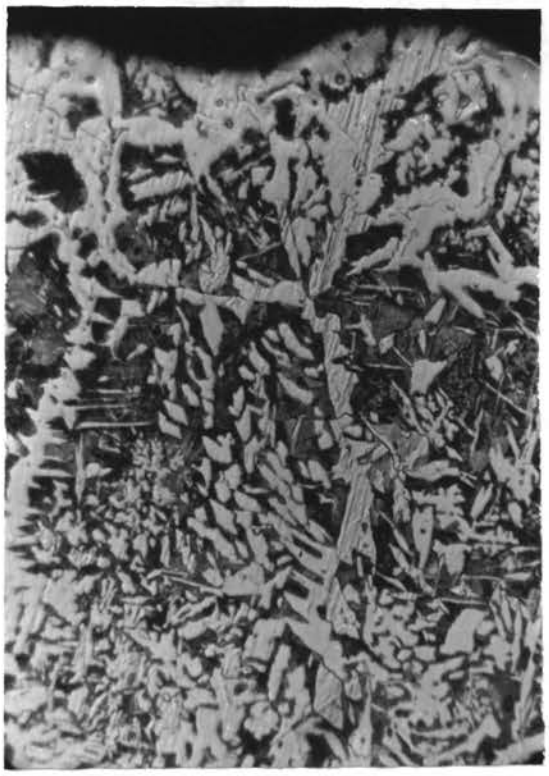

A. Carburized surface to left side. This side was against a shell mold of silica sand.

B. Surface structure of right side. This side was against a shell mold containing silica sand and 30% +200 mesh magnetite.

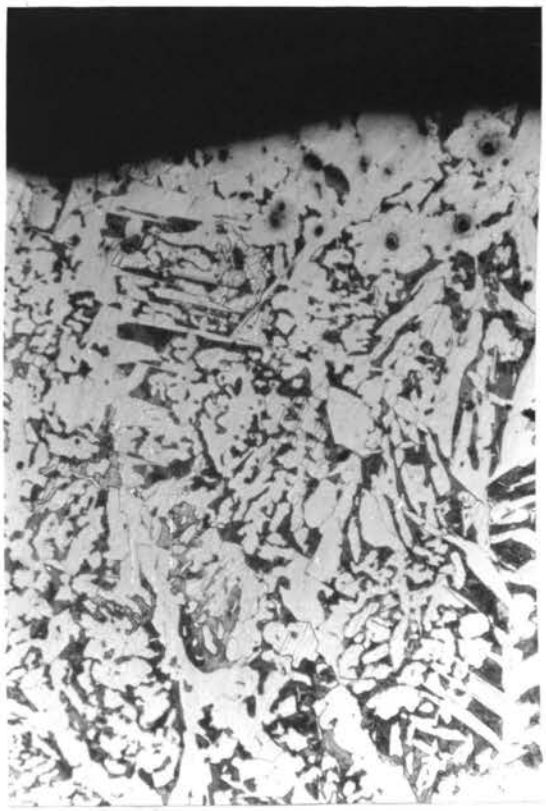

Figure 24. Photomicrographs (100X) of the surface on opposite sides of casting #41. Etchant 5% Nital.

A. Structure of bead on the surface of casting #6. Note carburization below defect.

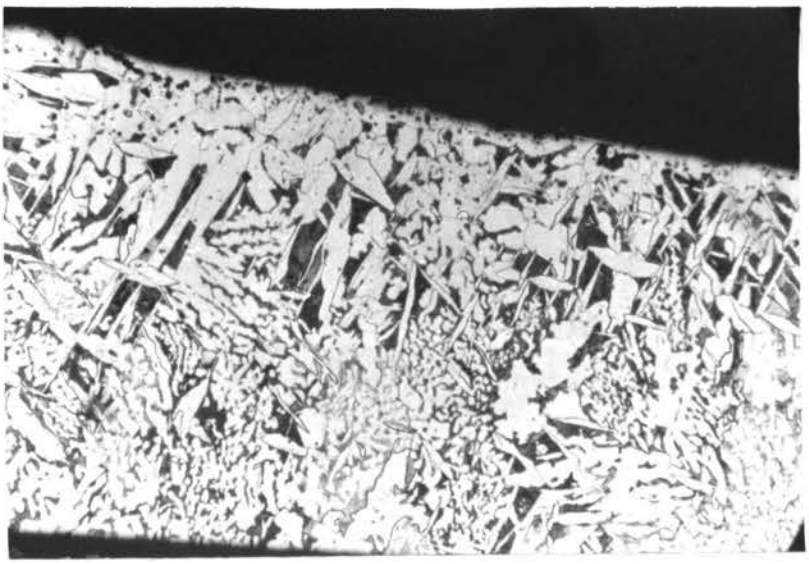

B. Normal surface structure of casting #6 in area where no beads occurred.

Figure 25. Photomicrographs (100X) comparing surface structures in casting #6. Etchant 5% Nital.

A. Casting #24.

B. Casting #18

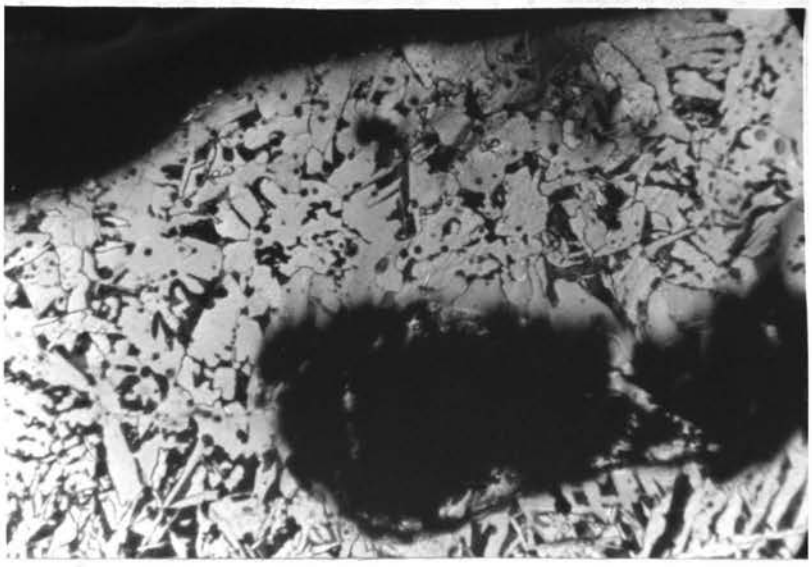

C. Casting #5

Figure 26. Photomicrographs (100X) showing structure of surface beads. Etchant 5% Nital. Note carburization below defect.

A. Casting #23. Example of carburization beneath the surface blow.

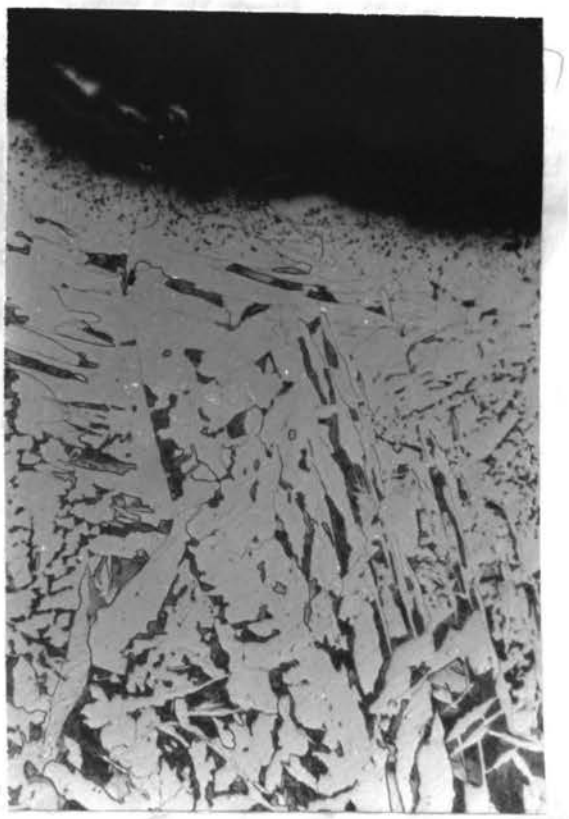

B. Casting #34. Normal structure beneath surface blow.

Figure 27. Photomicrographs (100X) of the surface structure of castings exhibiting the gas blow defect. Etchant 5% Nital.

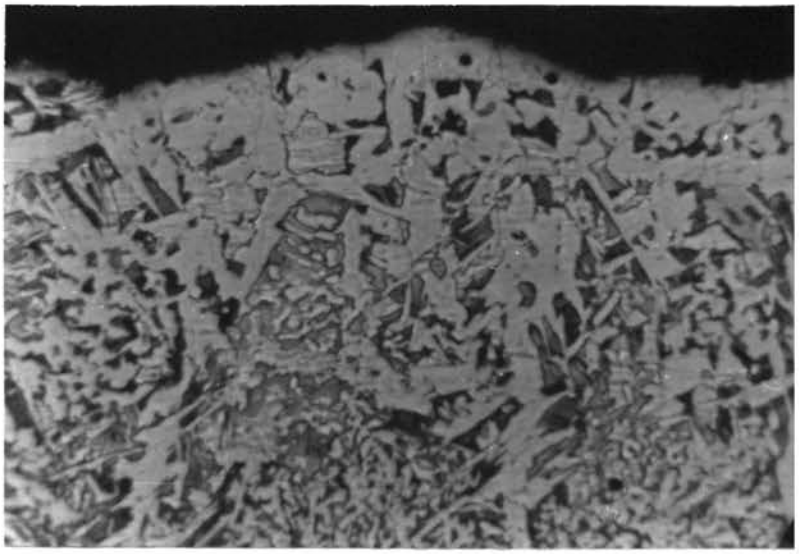

A. Casting #3

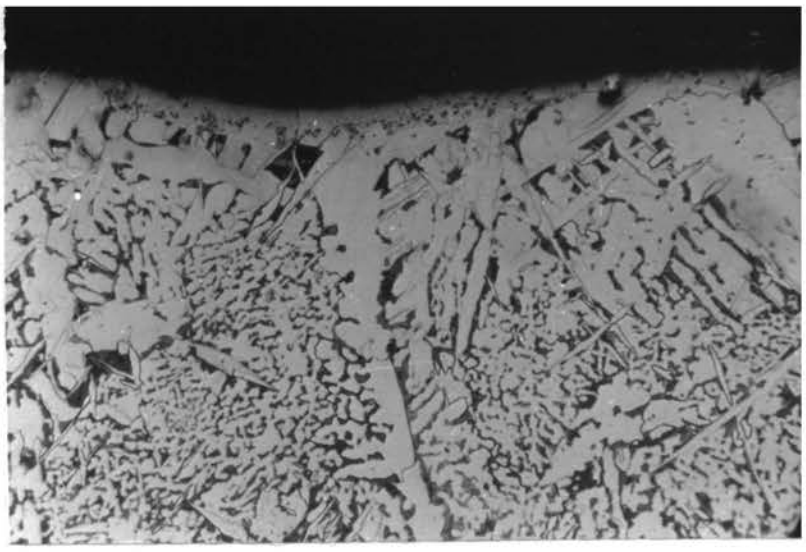

B. Casting #2

Figure 28. Photomicrographs (100X) of the surface structure of castings exhibiting no surface defects.

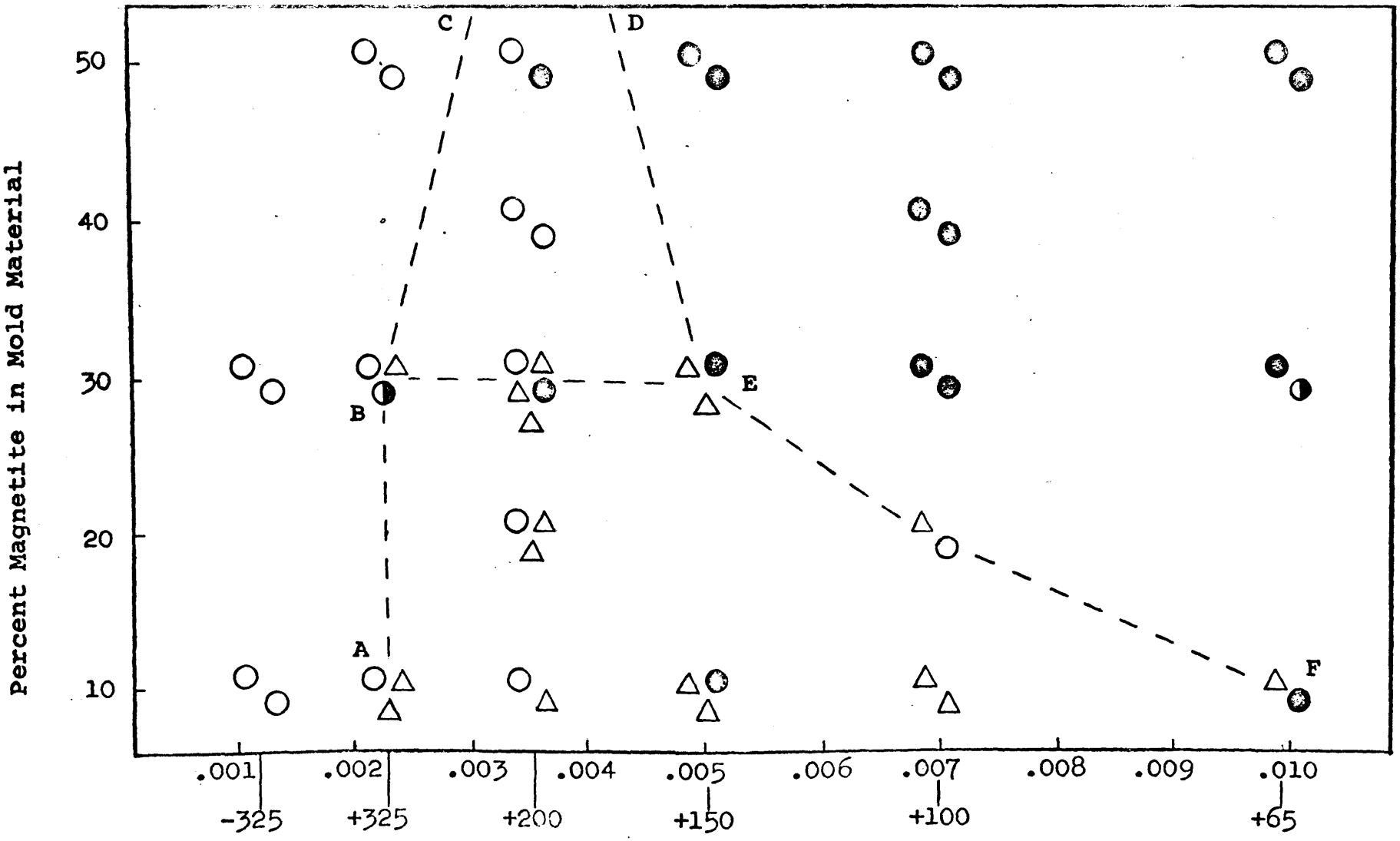

Figure 29. Rating of casting surfaces as a function of mold composition.
Acceptable Rejected - Beads Rejected - Blows

IV DISCUSSION OF RESULTS

For continuity in the presentation of the results of this investigation the identification of the surface defects resulting from mold expansion has already been described in Figure 22. Cowles[18,19] has established the effect of additives with lower expansion characteristics than silica in preventing expansion defects. The effect of the magnetite additions of this investigation cannot satisfactorily be explained in this manner when it is recalled that magnetite also eliminated the expansion defect when added to zircon shell molds. The expansion defect is less severe in the zircon molds because "zircon's low expansion (less than one-third that of silica) removes many of the problems encountered with silica sand."[40] The only value which could be found for the thermal expansion coefficient of magnetite[43] showed it to be approximately the same as the value for zircon. The fact that small additions (10%) of magnetite to silica eliminated the expansion defect and additions to zircon sand also eliminated the defect indicates that, although the smaller expansion of magnetite may contribute some thermal stability to a mix of magnetite and silica sand, the effect is minor.

The breakdown of the resin furnishes a source of carbon which combines with the available oxygen to produce a CO-CO_2 atmosphere. Carburization of low carbon steels cast in shell molds has been reported several times,[24-27] therefore, the carburization of the castings made in regular silica and zircon shell molds was to be expected. Additions of magnetite to the mold almost completely eliminated carburization of the surface which indicated that more oxygen was available for the combustion of the carbon residue. If this is the case, magnetite, Fe_3O_4, would have to contribute the oxygen.

Casting temperatures in this investigation were approximately 1600°C. The mold material adjacent to the interface will approach this temperature. The diagram of Darken[35] (Figure 2) shows that at this temperature, the stable phases would be an iron silicate melt and solid silica. The formation of an iron silicate melt in an oxidizing atmosphere has been described by the formation of FeO on the surface of steel castings and the reaction of FeO with SiO_2 (Figure 4). In the case of the molds containing magnetite, a reduction of the Fe_3O_4 to FeO might occur. This is considered possible when it is recalled that the reducing nature of shell sand molds has been

found to inhibit the formation of FeO by oxidation of iron.[39] Van Vlack, Wells, and Pierce[45] determined that the shell mold produced strongly reducing conditions. The reduction of Fe_3O_4 to FeO would also agree with the hypothesis that carburization is eliminated in these castings because of the oxygen made available by the magnetite for the combustion of carbon.

With reference to the preceding paragraph, if FeO is formed by the reduction of Fe_3O_4, reactions between the FeO and SiO_2, would occur within the mold material. This could result in the presence of a liquid phase at temperatures as low as 1200°C (Figure 4).

Darken[35] describes the equilibrium between the magnetite plus silica and the fayalite plus silica regions of the diagram (Figure 2) by the reaction below.

$$3(2FeO\text{-}SiO_2) + 2CO_2 = 2Fe_3O_4 + 3SiO_2 + 2CO$$

If the CO_2/CO ratio and the temperature were in favor of this reaction proceeding to the left, fayalite would be formed by this reaction within the mold. The fayalite, $FeSiO_4$, melts at approximately 1200°C (Figure 4).

Evidence that a chemical reaction between the constituents of the mold did occur was obtained from the

mold samples collected after casting. Representative photographs of these samples are shown in Figure 30. These layers were adjacent to the casting surface and were not magnetic. The original mold material containing magnetite was, of course, magnetic. Reaction layers of this type were present only in the molds which contained magnetite. The samples shown in Figure 30 are identical in appearance to the "sinter layer" resulting from the interface reaction between iron oxide and silica reported by Savage and Taylor.(36)

Although reference has been made to previous research concerning the reaction with silica, no mention has been made of the possible reactions with zircon ($ZrO_2 \cdot SiO_2$). The reaction layer was observed in the molds containing zircon sand and magnetite (Figure 30). Iron-oxide does flux ZrO_2 as seen in Figure 31. Apparently similar reactions to those previously discussed for silica sand occur in the molds containing magnetite and zircon sand.

If chemical reactions between the magnetite and silica or zircon would result in a liquid phase, this liquid could allow the expansion of the individual sand grains to occur without producing stresses in the mold. The elimination of these stresses would prevent the mold wall

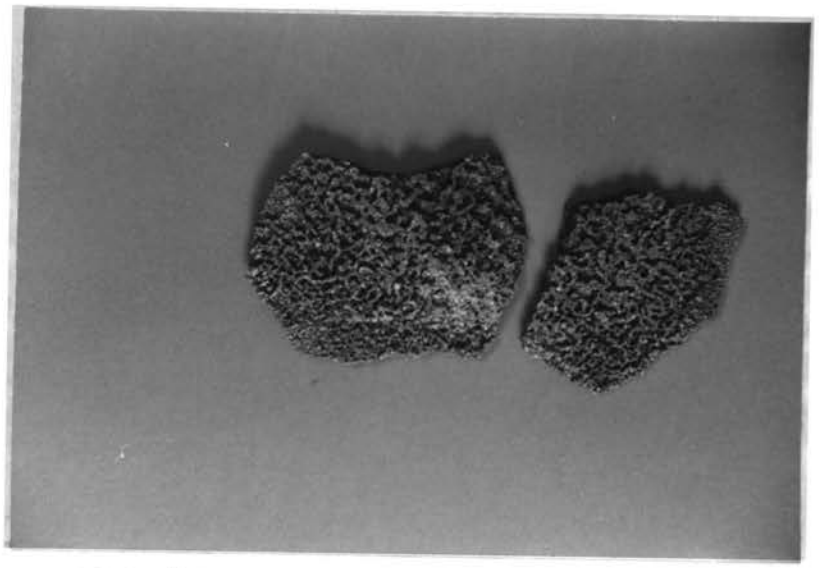

A. Mold #31, silica sand plus magnetite.

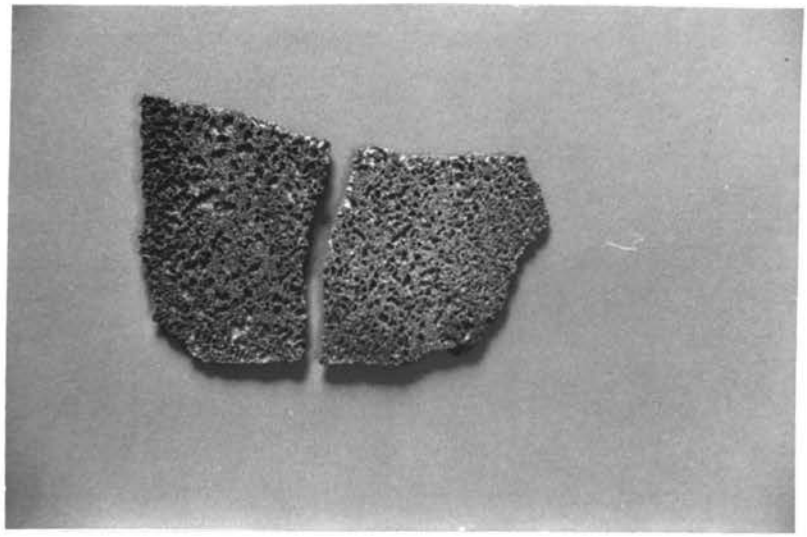

B. Mold #52, zircon sand plus magnetite.

Figure 30. Photographs of mold material (after casting) at metal interface.

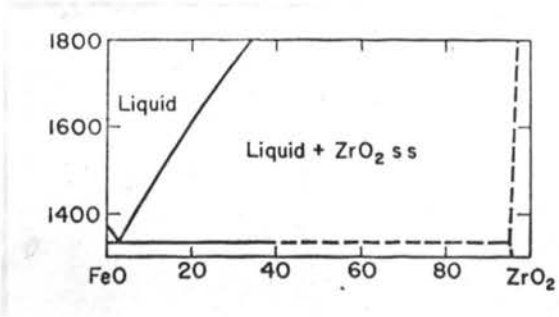

Figure 31. Equilibrium diagram of the system $FeO-ZrO_2$.(45)

from distorting, thus preventing the expansion defect. A model illustrating how a liquid phase would permit the individual grain expansion is shown in Figure 32.

The reaction layers observed in this investigation were about 1/8" thick. Whether or not less complete reactions occurred at greater distances from the interface is not known, however, it is doubtful the reaction zone ended abruptly.

The temperature of the molten steel entering the mold was above the melting point of magnetite (1538°C). This fact can be used to explain the pickup of magnetite from the mold resulting in beads on the surface of the casting. As the liquid metal entered the mold, fusion of some of the magnetite particles located on the inner surface of the mold occurred concurrent with the formation of a thin skin of solidified metal. The pickup of magnetite was only observed on the larger particles because these particles would have more surface area in contact with the steel. The smaller particles are apparently "shielded" by the refractory sand. A greater percentage of magnetite would represent a greater possibility for a group of magnetite particles to occur at the surface. This condition would be more suitable for the fusion of magnetite. The fusion

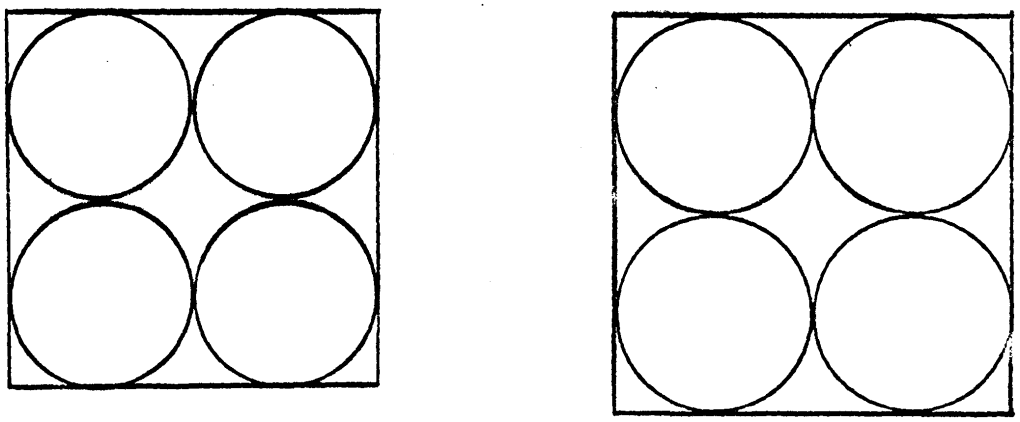

A. Expansion of individual particles necessitates the allotment of more space for the accommodation of the particles.

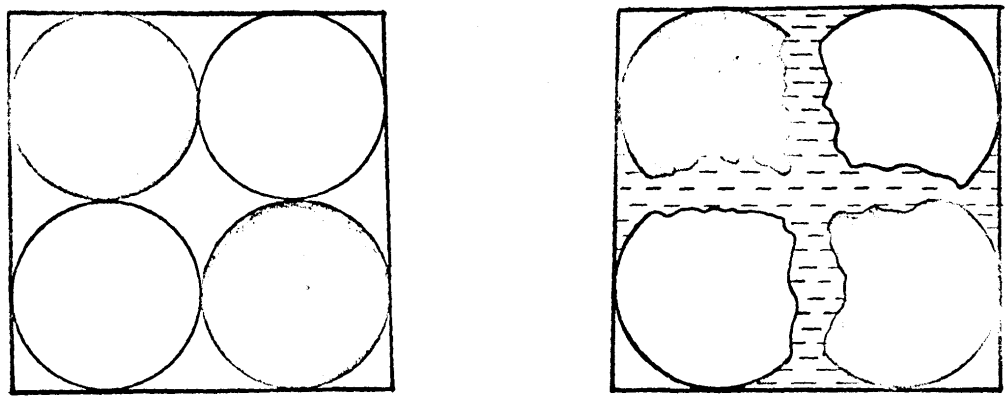

B. Liquid reaction product permits expansion to occur within the original space.

Figure 32. Model illustrating expansion in presence of liquid phase.

○ Sand particle ● Magnetite particle ⩦ Liquid

of magnetite particles at the surface would be dependent on a relation between the size of the magnetite particles and the size of the sand grains.

The voids exhibited in the microstructures of the beads are probably a result of gas porosity and solidification shrinkage. It is possible that the solid material removed from some of the holes was a slag formed by the impurities in the magnetite. Carburization of the surface below the beads indicates that fusion of the magnetite particles occurred before the carbon from the resin had a chance to burn off. This would mean the carbon deposited on the magnetite would be trapped as the liquid steel partially surrounds the magnetite particle.

A decrease in the permeability of the mold would be expected to result from the addition of fine particles to the mold. Permeability is a measure of the continuous voids and small particles would tend to locate in the natural voids formed by the larger sand particles. It was also determined (Appendix II) that the resin content of the coated magnetite particles increased with decreasing size. A combination of the increased gas evolution (increased resin content) and decreased permeability adequately explains why the gas blows were formed on the castings made

in shell molds containing the smaller magnetite particles.

The limited observations which have been made from the castings made from zircon and magnetite shells substantiate the explanations for the occurrence of the surface defects associated with magnetite additions.

V CONCLUSIONS

1. Shell molds can satisfactorily be cured using induction heating when magnetite particles are present in the mold mix.

2. It is possible to obtain excellent surfaces on low carbon steel castings cast in shell molds containing magnetite additions.

3. When steel is cast into shell molds composed of magnetite and silica or zircon sand, chemical reactions occur within the mold material. The reaction is most pronounced at the mold-metal interface. It is probable that an iron-silicate melt is formed by the reactions.

4. Additions of magnetite in the shell molds eliminated the occurrence of expansion defects on the surface of the castings. A possible explanation of this effect is the formation of a liquid phase within the mold material.

5. There was almost complete absence of surface carburization when magnetite additions were made to the shell molds.

6. The addition of magnetite to the shell molds was responsible for the appearance of two different surface defects. Larger particles were fused by the liquid metal entering the mold and appeared as surface beads on the

surface of the casting. The addition of smaller particles resulted in gas blows on the casting surfaces due to increased gas evolution and decreased permeability of the mold material.

7. The particle size and percentage of the magnetite added is critical with respect to the prevention of surface defects associated with the magnetite additions. The limits of size and percentage of magnetite additions which would yield a satisfactory casting is expected to change with changes in the size and distribution of the sand particles.

BIBLIOGRAPHY

1. FLINN, R.A. (1963) "Fundamentals of Metal Casting." Addison-Wesley, Reading, Mass., p. 3.

2. AMES, B.N., DONNER, S.D., and KAHN, N.A. (1952) "The Shell Molding Process." Foundry, Vol. 80, June, p. 111.

3. SIMONDS, H.R. (1957) "Concise Guide to Plastics." Reinhold, New York, p. 4.

4. REPORT OF THE INSTITUTE OF BRITISH FOUNDRYMAN (1952) "Synthetic Resin Corebinders." American Foundryman, Vol. 21, Feb., p. 51.

5. DORFMUELLER, A. (1962) "How to Choose a Binder." Foundry, Vol. 90, April, p. 54 - 59.

6. PARKES, E. (1964) "A Survey of Developments in Synthetic Resin Binders for the Manufacture of Cores." British Foundryman, Vol. 57, p. 329 - 335.

7. REPORT OF THE INSTITUTE OF BRITISH FOUNDRYMAN (1963) "A Statement of the Existing Knowledge on the New Core-Making Processes." British Foundryman, Vol. 56, p. 100 - 108.

8. ALBANESE, J. (1960) "Shell Mixing Processes and Equipment". AFS Transactions, Vol. 68, p. 225 - 228.

9. CAPEHART, W.C. (1959) "New Foundry Resins and Application Techniques for Shell Molds and Shell Cores." AFS Transactions, Vol. 67, p. 329 - 336.

10. CLIFFORD, M.J. (1963) "Review of Modern Coremaking Processes." Iron and Steel, Vol. 36, p. 308 - 313.

11. VALYI, E.I. (1954) "Developments in Shell Molding." American Foundryman, Vol. 25, May, p. 138 - 143.

12. GOULD, D.F. (1959) "Phenolic Resins." Reinhold, New York, 213 pages.

13. WRIGHT, R.L., Personal Communication.

14. COMMITTEE 8-N, AMERICAN FOUNDRYMEN'S SOCIETY (1958) "Shell Molding Survey." AFS Transactions, Vol. 66, p. 324 - 327.

15. TAYLOR, H.F., FLEMINGS, M.C., and WULFF, J. (1959) "Foundry Engineering." Wiley and Sons, New York.

16. OETTINGER, J.F. (1959) "Shell Molding." Modern Castings, Vol. 36, July, P. 130.

17. FLINN, R.A. (1963) "Fundamentals of Metal Casting." Addison-Wesley, Reading, Mass., p. 161.

18. COWLES, R.J. (1962) "Studies Leading to the Elimination of Deformation and Cracking in Shell Molds and Cores During Casting." AFS Transactions, Vol. 70, p. 993 - 1001.

19. COWLES, R.J. (1963) "Studies of Aggregate Blends, Additives, and Pretreatments to Eliminate Thermal Deformation and Cracking in Shell Molds and Cores During Casting." AFS Transactions, Vol. 71, p. 794 - 799.

20. RABE, R.A. (1958) "Study of High Temperature Properties of Shell Molds." AFS Transactions, Vol. 66, p. 484 - 494.

21. COWLES, R.J. (1959) "Introduction of Tentative Hot Shell Deformation Test." AFS Transactions, Vol. 67, p. 513 - 516.

22. SALZBERG, H.K. and GREAVES, J.J. (1960) "Phenolic Resin Bond in Solid Sand Cores." Modern Castings, Vol. 38, July, p. 101 - 110.

23. STEEL FOUNDERS SOCIETY OF AMERICA (1960) "Organic Bonding of Steel Foundry Sands." Journal of Steel Castings Research, No. 18, p. 12 - 15.

24. THIEME, J. (1964) "Defects in Shell Molded Carbon Steel Castings." Journal of Steel Castings Research, No. 35, p. 6 - 8.

25. BEHRING, J.A. and HIENE, R.W. (1960) "Surface Defects on Shell Molded Castings." Modern Castings, Vol. 37, Feb., p. 58 - 66.

26. JAMES, D.B. and MIDDLETON, J.M. (1959) "An Examination of Methods to Improve the Surface Finish of Shell Molded - Low Carbon Steel Castings". The British Foundryman, Vol. 52, p. 387 - 395.

27. STEEL FOUNDER'S SOCIETY OF AMERICA (1964) "The Shell Molding Process for Plain Carbon and Low Alloy Steel Castings." Journal of Steel Castings Research, No. 32, p. 12 - 16.

28. JACKSON, R.S. and GLICK, W.W. (1959) "Resin and Sand Economy, and Surface Finish in Shell Moulds." British Foundryman, Vol. 52, p. 53 - 61.

29. OWEN, W.H. (1958) "Forsterite Offers Advantages as Shell Mold Material." Foundry, Vol. 86, Feb., p. 134 - 137.

30. POWELL, R.G. and TAYLOR, H.F. (1958) "Shell Molding for Steel Castings." Modern Castings, Vol. 34, p. 403 - 408.

31. NAVARRO, J. and TAYLOR, H.F. (1956) "Inorganic Binders Solve Shell Molding Problems". AFS Transactions, Vol. 64, p. 625 - 635.

32. POWELL, R.G. and TAYLOR, H.F. (1961) "Develops New Shell Molding Process". Foundry, Vol. 89, Nov., p. 88 - 92.

33. RIGGAN, H. (1942) "The Use of the Hot Strength Test as a Tool for Controlling Core Mixtures." AFS Transactions, Vol. 50, p. 1185 - 1197.

34. DIETERT, H.W., DOELMAN, R.L., and BENNETT, R.W. (1944) "Mold Atmosphere Control". AFS Transactions, Vol. 52, p. 1053 - 1071.

35. DARKEN, L.S. (1948) "Melting Points of Iron Oxides on Silica; Phase Equilibria in the System Fe-Si-O as a Function of Gas Composition and Temperature." Journal of American Chemical Society, Vol. 70, p. 2046 - 2053.

36. SAVAGE, R.E. and TAYLOR, H.R. (1950) "Fayalite Reaction in Sand Molds used for Making Steel Castings." AFS Transactions, Vol. 58, p. 564 - 577.

37. LEVIN, E.M., McMURDIE, H.F. and HALL, F.P. (1956) "Phase Diagrams for Ceramists." American Ceramics Society, Figure 63, p. 51.

38. COLLIGAN, G.A., VAN VLACK, L.H., and FLINN, R.A. (1958) "The Effect of Temperature and Atmosphere on Iron-Silica Interface Reaction." AFS Transactions, Vol. 66, p. 452 - 458.

39. COLLIGAN, G.A., VAN VLACK, L.H., and FLINN, R.A. (1961) "Factors Affecting Metal - Mold Reactions." Modern Castings, Vol. 39, Jan., p. 104 - 110.

40. AMERICAN FOUNDRYMEN'S SOCIETY (1962) "Molding Methods and Materials." Des Plaines, Illinois, 614 p.

41. ACME RESIN CORPORATION, Forest Park, Illinois, Private Correspondence.

42. W.S. TYLER COMPANY (1964) "Testing Sieves and Their Uses." Handbook 53, Cleveland, Ohio.

43. FOWLE, F.E. (1944) "Smithsonian Physical Tables." Smithsonian Institute, Washington, D.C., p. 224.

44. VAN VLACK, L.H., WELLS, R.G. and PIERCE, W.B. (1958) Reduction of Silica in Large Shell Molds." AFS Transactions, Vol. 66, p. 459 - 465.

45. LEVIN, E.M. and MeMURDIE, H.F. (1959) "Phase Diagrams for Ceramists - Part II." American Ceramic Society, Figure 1035, p. 14.

APPENDIX

APPENDIX I

SCREEN ANALYSIS OF SANDS

Screen analyses were performed on the silica and zircon sands. From the results of the screen analyses, the AFS Grain Fineness Number was calculated for each of the two sands. By definition, the AFS Grain Fineness Number is the average grain size, and it corresponds to the sieve number whose openings would just pass all the sand grains if all were of the same size. The data obtained from the screen analyses and the calculations of the fineness number are contained in Table I (silica sand) and Table II (zircon sand). Figure 33 serves to show the grain size distribution of the two sands.

Tyler Mesh Designation	Amount of 200 Gram Sample Retained Wt.	%	Multiplier	Product
35	0	0.0	30	-
48	2	1.0	40	40
65	9	4.5	50	225
100	62	31.0	70	2170
150	75	37.4	100	3740
200	32	16.0	140	2240
270	12	6.0	200	1200
Pan	4	2.0	300	600
	196	96.9		10215

$$\text{AFS Grain Fineness Number} = \frac{\text{total product}}{\text{total \% retained}}$$

$$= \frac{10215}{96.9} = 105$$

Table I Calculation of AFS Grain Fineness Number of the silica sand.

Tyler Mesh Designation	Amount of 200 Gram Sample Retained Wt.	%	Multiplier	Product
35	0	0.0	30	-
48	3	1.5	40	60
65	2	1.0	50	50
100	11	5.5	70	385
150	37	18.5	100	1850
200	77	38.5	140	5390
270	51	25.5	200	5100
Pan	12	6.0	300	1800
	193	96.5		14635

$$\text{AFS Grain Fineness Number} = \frac{\text{total product}}{\text{total \% retained}}$$

$$= \frac{14,635}{96.5} = 152$$

Table II Calculation of AFS Grain Fineness Number of the zircon sand.

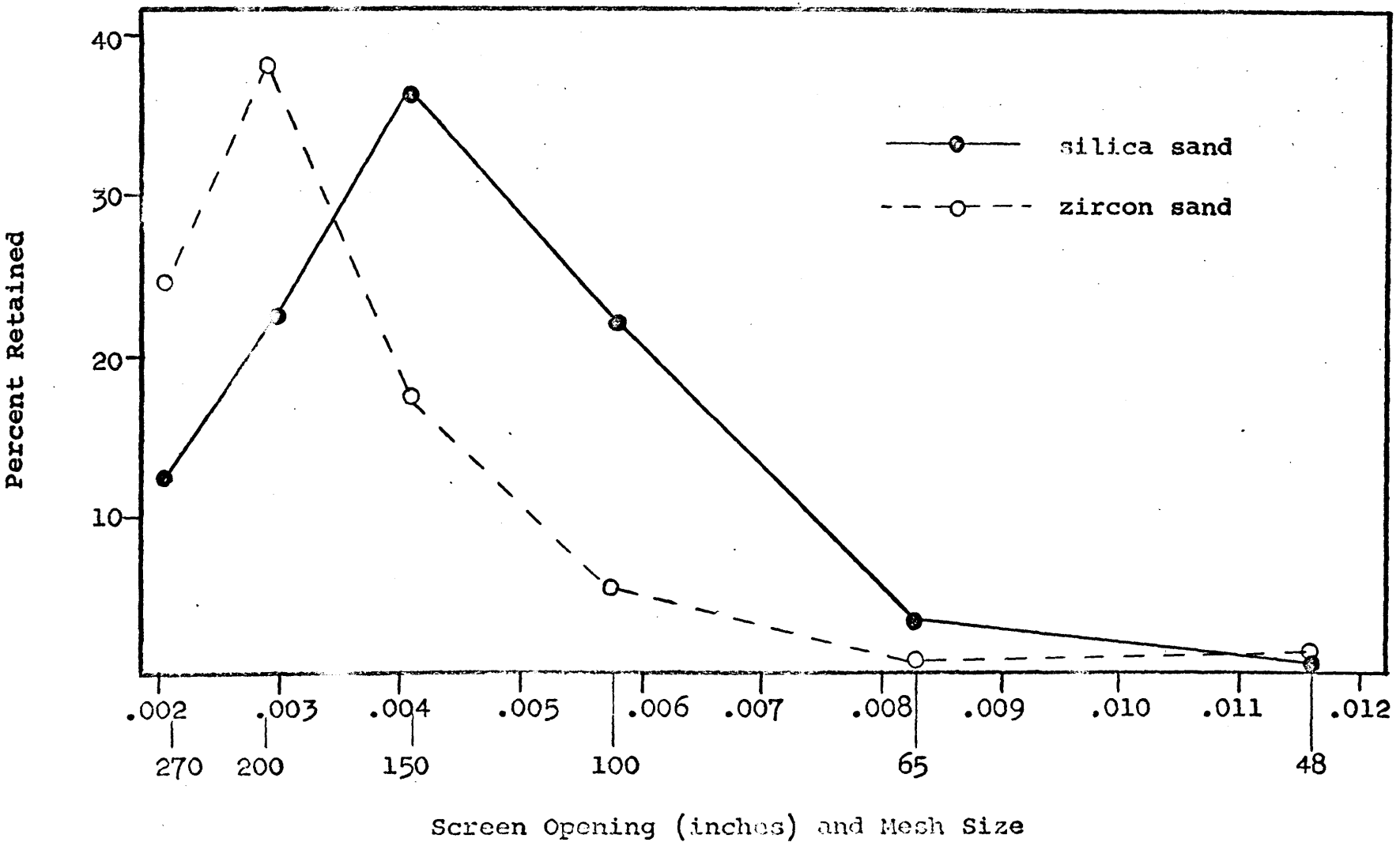

Figure 33. Size distribution of sand grains

APPENDIX II

RESIN CONTENT OF MAGNETITE

As stated previously, the magnetite was coated with 5.3 weight percent resin. At this stage the resin is soluble in alcohol. A sample from each of the magnetite particle sizes weighing approximately 50 grams was obtained. These samples were placed in separate 250 cc beakers into which alcohol was added to dissolve the resin coating. This mixture was stirred with a glass rod, the magnetite was allowed to settle, and the liquid was poured through a filter paper placed in a funnel. This process was repeated several times until the resin was completely dissolved as indicated by the absence of reddish-brown coloring of the alcohol. Alcohol was then used to transfer the magnetite into the filter paper. After several washings the magnetite and filter paper were allowed to dry and were weighed. The weight loss corresponded to the weight of the resin coating on the original 50 gram samples. The data obtained is shown in Table III and plotted in Figure 34. It is seen that as the particle size decreases, the resin content of the magnetite increases.

Particle Size	Avg. Diam.(in.)	Wt. Paper (g)	Wt. Fe_3O_4 (g)	Final Wt. Paper + Fe_3O_4 (g)	Wt. Loss (g)	% Resin	Area/Volume Ratio (6/0)
+65	.0099	2.29	50.15	51.77	.67	1.34	605
+100	.0070	2.29	50.30	51.10	1.49	2.97	855
+200	.0035	2.27	50.65	50.57	2.35	4.65	1710
+325	.0023	2.29	50.59	49.81	3.07	5.55	2600
-325	----	2.30	50.22	48.50	4.02	8.0	----

Table III Results of the determination of the resin content of magnetite.

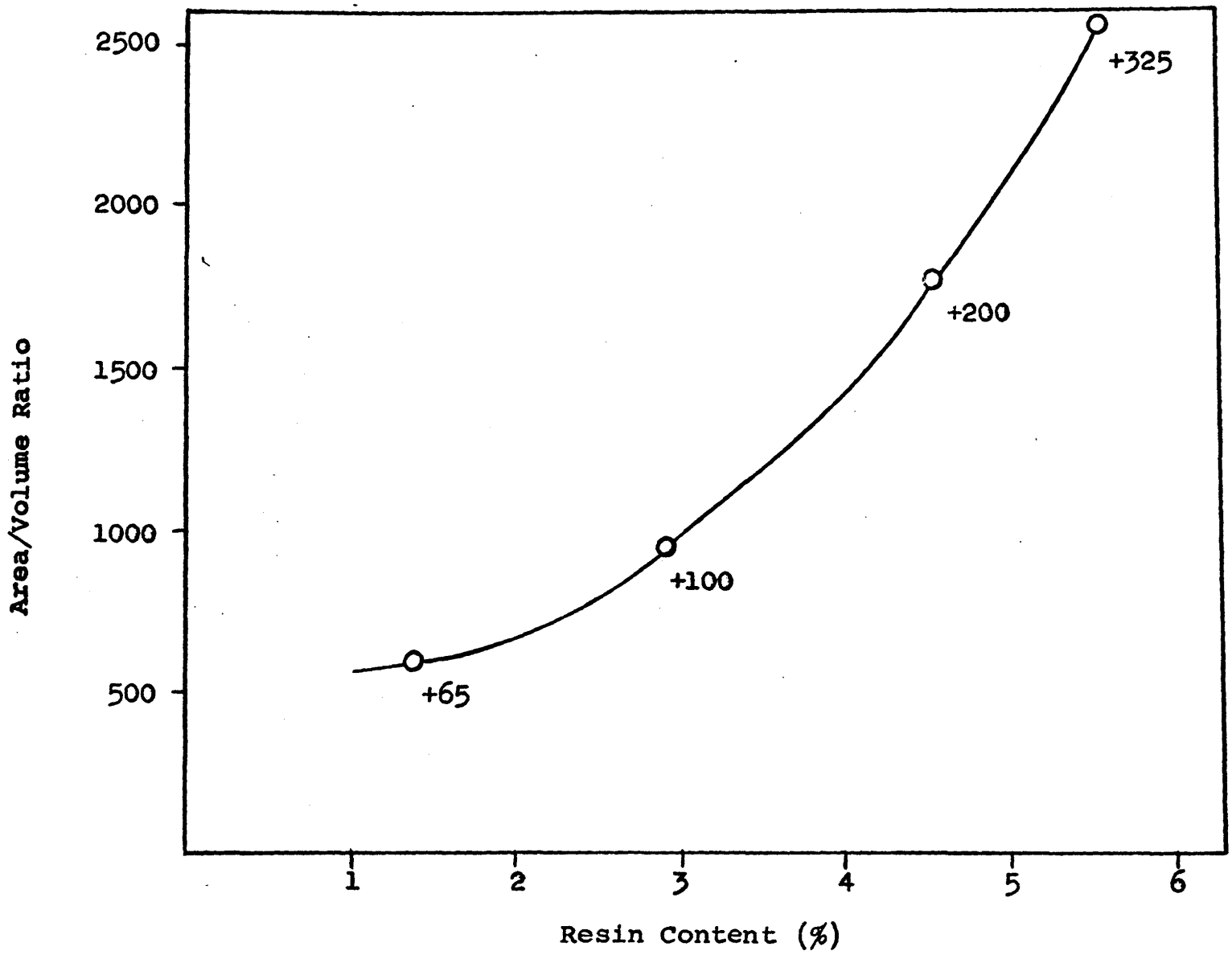

Figure 34. Variation of resin content with magnetite particle size.

APPENDIX III

COMPLETE DESCRIPTION OF CASTINGS

Casting # Mold #	Mold Composition	Surface Quality Acc.	Rej.	Surface Defect
1	S, 30% M(+100)		X	Beads
2	S, 30% M(+200)	X		-
3	S, 10% M(+100)	X		-
4	S, 30% M(-325)		X	Blow
5	S, 50% M(+65)		X	Beads
6	S, 50% M(+65)		X	Beads
7	S, 30% M(+150)	X	X	Beads
8	S, 10% M(+65)	X	X	Beads
9	S, 10% M(-325)		X	Blow
10	S, 10% M(+325)	X		-
11	S, 10% M(+200)	X		-
12	S, 10% M(+150)	X	X	Beads
13	S, 30% M(+325)	X	X	Beads Blow
14	S, 30% M(+100)		X	Beads
15	S, 10% M(+325)	X		-
16	S, 10% M(+200)		X	Blow
17	S, 30% M(+200)	X	X	Blow
18.	S, 30% M(+65)		X	Beads

Table IV-A Complete description of castings
S = Silica sand, Z = Zircon sand, M = Magnetite

Casting # Mold #	Mold Composition	Surface Quality Acc.	Rej.	Surface Defect
19	S, 10% M(-325)		X	Blow
20	S, 30% M(+65)		X	Beads Blow
21	S, 30% M(+150)	X		-
22	S, 30% M(+325)		X	Blow
23	S, 30% M(-325)		X	Blow
24	S, 50% M(+100)		X	Beads
25	S, 50% M(+200)		X	Beads
26	S, 10% M(+150)	X		-
27	S, 10% M(+100)	X		-
28	S, 50% M(+200)		X	Beads Blow
29	S, 50% M(+150)		X	Beads
30	S, 50% M(+100)		X	Beads
31	S, 50% M(+150)		X	Beads
32	S, 50% M(+325)		X	Blow
33	No Casting			
34	S, 50% M(+325)		X	Blow
35	S		X	Expansion
36	S		X	Expansion
37	S		X	Expansion
38	S		X	Expansion

Table IV-B Complete description of castings
S = Silica sand, Z = Zircon sand, M = Magnetite

Casting # Mold #	Mold Composition	Surface Quality Acc.	Rej.	Surface Defect
39	S		X	Expansion
40	S		X	Expansion
41 (R)	S, 30% M(+200)	X	X	Beads
41 (L)	S		X	Expansion
42	S, 40% M(+100)		X	Beads
43	S, 40% M(+100)		X	Beads
44	S, 20% M(+200)	X	X	Blow
45	S, 40% M(+200)		X	Blow
46	S, 20% M(+200)	X		-
47	S, 20% M(+100)	X	X	Blow
48	S, 40 M(+200)		X	Blow
49	Z		X	Expansion
50	Z	X	X	Expansion
51	Z, 30% M(+150)	X	X	Beads
52	Z, 30% M(+150)		X	Beads
53	Z, 30% M(+200)		X	Blow
54	Z, 30% M(+200)		X	Blow

Table IV-C Complete description of castings
S = Silica sand, Z = Zircon sand, M = Magnetite

VITA

The author was born April 11, 1941 in Cape Girardeau, Missouri. He received his elementary and secondary education in the public schools of Cape Girardeau, graduating from Central High School in May of 1958. He entered the Missouri School of Mines and Metallurgy in September, 1958, and received the B.S. Degree in Metallurgical Engineering in May, 1962.

After being employed by the Bethlehem Steel Corporation as a Project Metallurgist for 2½ years, he returned to the University of Missouri at Rolla in September, 1964 to pursue the Master of Science Degree in Metallurgical Engineering. He held the position of Graduate Teaching Assistant in the Department of Metallurgical Engineering for three semesters.